Sightline Control Basics for Geo-Pointing and Locating - Part 1

by

Peter J. Kennedy

Copyright© 2019 Peter J. Kennedy

Introduction: This course discusses geo-pointing and locating. It is organized as three topics; the first addresses generic sightline control (SLC). As geo-locating requires geo-pointing and pointing requires maintaining a stable line of sight (LOS) to a targeted object or area, then an understanding of SLC is important. The second topic focusses on the geo-pointing problem given a stable sightline to the object to be geo-located. Finally the basics of geo-location, using direct and image geo-registration, are described. Many SLC sections require some background in control theory as well as mathematical operations with vectors and matrices. It is not essential to follow all the math but it is important to understand the need for it and how it plays into an overall solution. Pointing design should follow a top down design procedure; beginning with requirements through HW and SW design and implementation. However given cost and schedule constraints, one is often forced into an off the shelf design with compromised performance. Understanding the design requirements, however, should not be compromised so related performance can be quantified and improved in future designs. The purpose of the course is to lay a framework for understanding this design process. There should be sufficient math detail for those interested at the equation level but hopefully adequate course structure for those not interested to still follow the overall design process. The course has a two part structure; Part 1 covers SLC basics and geo-pointing and Part 2 provides a brief review of Part 1 followed by a focus on geo-locating and Part 3 is a shorter description of sensor coverage geometry and characteristics for geo-location.

1.0 Line of Sight Definition and Performance Overview [1,2, 3]

The line of sight is defined as a vector between points on an observation platform and an observed target location in an inertial referenced coordinate frame. Figure 1.0 illustrates a typical pointing scenario.

https://www.pexels.com/photo/quadcopter-flying-on-the-skey-1034812/ archived on 20 May 2018 at the Wayback Machine

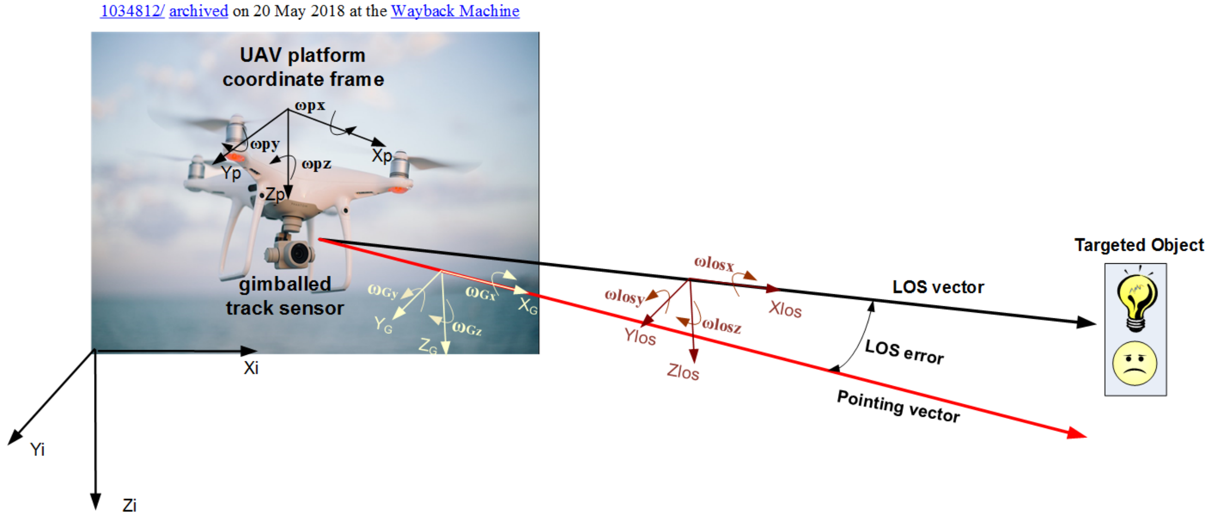

Figure 1.0 LOS Pointing Geometry

Copyright© 2019 Peter J. Kennedy

When discussing basic pointing control concepts, the inertial reference frame can be considered a general flat earth coordinate frame with motion constrained by the laws of inertia. As the course focus transitions to geo-pointing and location, this frame will be the North-East-Down (NED) coordinate frame defined in Section 8.0. The observer (i.e. a sensor) is required to maintain a target track providing its relative location based on a performance accuracy requirement. Sensors are aligned to the inertial stabilization sensor reference establishing the sightline or bore-sight within a gimbal structure capable of rotating about multiple axes. The gimbal is mounted to a stationary or moving platform. Sightline control (SLC) can be considered a two part problem:

- (1) LOS Point/Track: LOS pointing based on sensor performance over a specified the LOS platform to target kinematic envelope. It must meet pointing accuracy required for tracking and accurate location of a target
- (2) LOS Stabilization: LOS stabilization isolates the sensor from platform motion to stabilize the operating environment; rejecting disturbances due to platform motion to achieve the desired track/pointing accuracy. The control system isolating the sensor LOS vector from angular motion is: Stabilizing the LOS.

Pointing error is the difference between the actual LOS orientation and the sensor pointing vector to the target. Error is a function of inherent sensor pointing error, platform motion/vibration residual error, and often the atmosphere. Error sources are characterized in the 'error budget' with platform motion ('own ship motion') often driving performance.

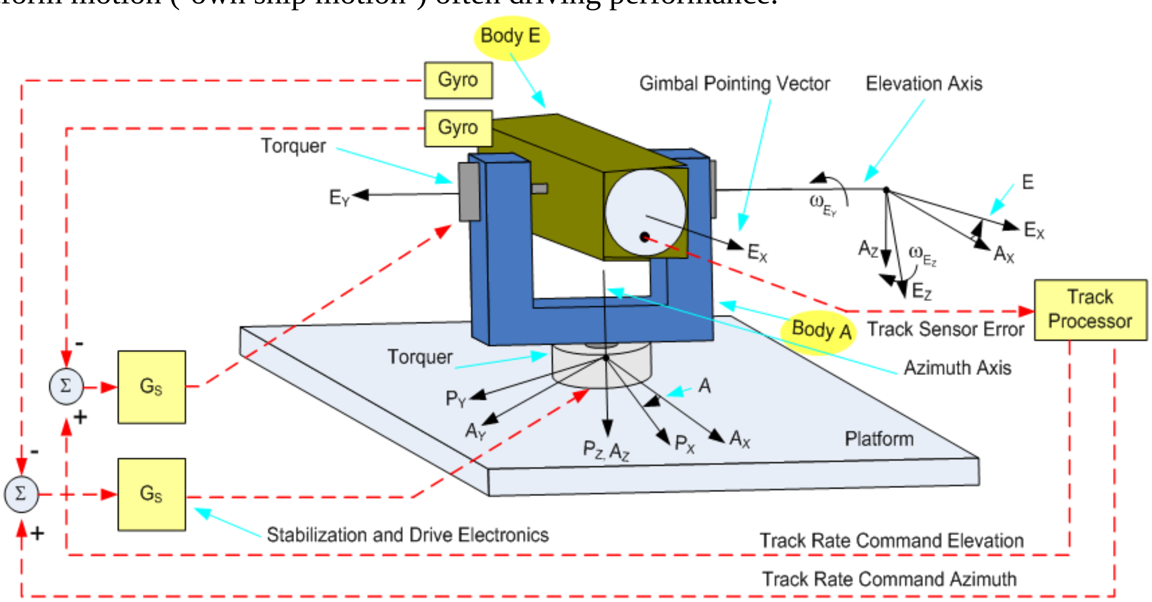

Figure 2.0 Simple 2-axis Elevation over Azimuth Gimbaled Track Sensor Geometry

Figure 2.0 illustrates a simple two axis elevation over azimuth (el/az) gimbal design. The outer body rotates in a horizontal plane relative to the base; termed azimuth rotation. The inner body rotates in a vertical plane relative to azimuth; termed elevation rotation. A coordinate frame is

 Copyright© 2019 Peter J. Kennedy

attached to each rotating axis body; as shown the inner el coordinate frame x-axis is the pointing axis. As shown, sensor and gyros are mounted directly on Body E with LOS motion defined by the inner el axes. Direct drive motors are used to control axis rotation; they will decouple axes inertia from base motion except for friction. The LOS and elevation inner body coordinate frames are coincident; gimbal elevation is LOS elevation; LOS cross elevation (XEL) is the rotation axis orthogonal to the LOS elevation axis (y) and the LOS pointing axis (x). So it is important to note that the rotation axes are azimuth outer and elevation inner while the LOS axes are cross elevation and elevation. Elevation LOS and rotation are the same but cross elevation is approximately azimuth*cos(E). At E=0° azimuth and cross elevation are equal; At E=90°, all 2-axis gimbal designs have a NADIR condition (Body E in Figure 2.0 points straight up) meaning from the definition of XEL, there is a singularity or division by zero and the azimuth axis control demand grows unbounded. Physically the XEL rotation axis is lost resulting in the condition termed 'gimbal lock'.

Many 2-axis designs use mirrors, with the sensor package located below the gimbal base. This reduces payload size, weight, and power (SWaP) but also adds complexities unique to mirrors discussed later. Multi-Axis gimbal geometries > 2 offer the potential for improved pointing performance benefitting from:

- Limited travel also limits disturbance geometry dependence to small angles
- All inner LOS axes protected from environment; no environmental seals/seal friction required.

A 3-axis design with an inner axis mounted on the elevation body rotating in XEL can solve the NADIR issue. A general control configuration for a multi-axis gimbal design has the inner axes driven by track sensor error; stabilize about inner axes; outer axes follow inner axes. Another consideration is as payload size increases; size and weight become prohibitive for direct mount on an inner gimbal. Payloads will require waveguides or a periscopic optical path and steering mirrors mounted to inner axes. When using a long optical path; it is best to integrate the final LOS control precision beam steering components as the last pointing elements in the gimbal optical path; otherwise they can:

- impact diameter of optical path, vignette sensor field of view unless path diameter is increased to account for beam motion
- Compromise overall LOS pointing as they will drive inner axes after the precision beam steering elements; resulting in LOS axis coupling

Figure 3.0 illustrates a high level SLC control system architecture and the interaction between key elements

 Copyright© 2019 Peter J. Kennedy

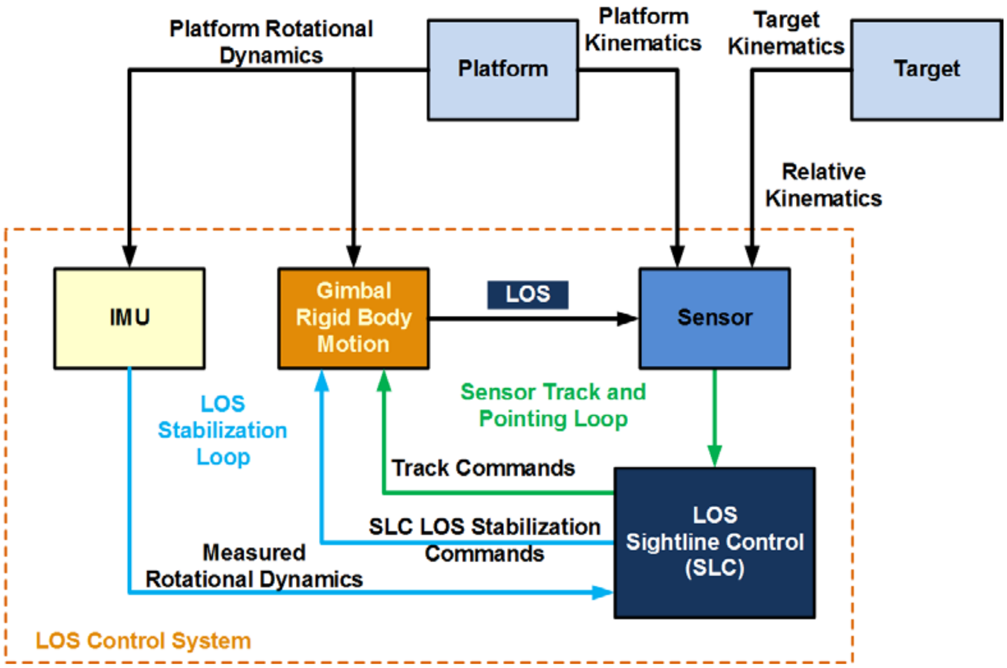

Figure 3.0 High Level SLC System Architecture

The primary input motion drivers are the target and platform. The track sensor provides the information for the track and pointing control loop based on the target to platform kinematics (green). The inertial measurement unit (IMU) measures the angular rate motion of the platform to drive the LOS stabilization control loop (blue). An IMU consists of 3 gyros measuring angular rates about 3 orthogonal axes (i.e. x, y, z) axes defined by the IMU and 3 accelerometers measuring linear acceleration along each axis. The track loop is the outer low bandwidth servo loop while the stabilization loop is the inner high bandwidth servo loop. Controlling the relative angular motion, direct or induced, between the platform and each LOS axis is critical to stabilization; disturbance attenuation is primarily an inverse function of loop gain or bandwidth. LOS and gimbal motion is characterized by the 'Rigid Body' gimbal dynamics (as opposed to structural flexure that also needs to be addressed) which must be modeled as part of the design process. In simplified control loop block diagrams the Rigid Body is equivalent to 1/J; J being a characteristic rotating axis inertia. In an actual application, it is a set of vector equations that describe the motion of a rigid body in 3 dimensions; to be described in Section 3.0. The key to SLC is disturbance rejection which equates to LOS stabilization. A simple illustration mapping of disturbance rejection to elements of a SLC system is shown in Figure 4.0 using the simple 2-axis gimbal from Figure 2.0

 Copyright© 2019 Peter J. Kennedy

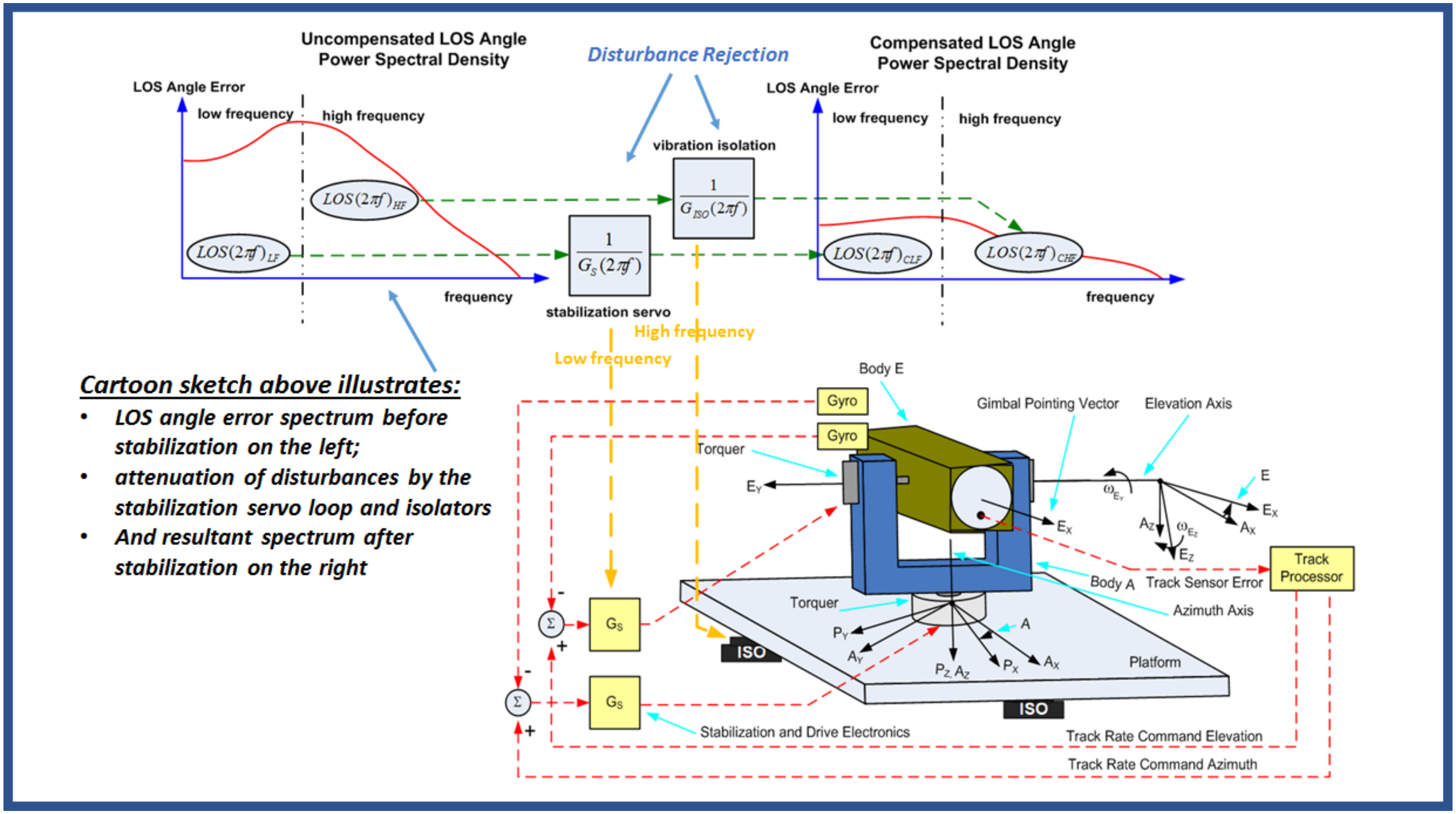

Figure 4.0 SLC System Disturbance Rejection

 Copyright© 2019 Peter J. Kennedy

The cartoon sketch in the upper portion of the figure illustrates the disturbance rejection objective. The LOS angle error spectrum before stabilization is on the left; followed by attenuation of disturbances by the stabilization servo loop and isolators and finally the resultant spectrum after stabilization on the right. The stabilization servo loop handles lower frequency disturbances. Gain (i.e. G_S) equates to BW so higher bandwidth provides better attenuation limited by power, noise, and servo stability constraints. In the digital world higher bandwidth equates to a higher sample frequency probably > 1 KHz and 5 KHz typical. Latencies (i.e. serial links) are a potential source of significant error. High frequency disturbances usually require mechanical isolation if significant to performance; resonances are always there; just where. Disturbance error is characterized in terms of jitter and bias or offset. Jitter is short term deviation about a zero mean. Bias is a longer term error, often due to mounting/component misalignment. Jitter deviates about this bias or offset. For design, bias and jitter are quantified via error allocation (desired or predicted) distribution and a final error budget (final allocation after complete critical design phase). Figure 5.0 illustrates the physical phenomena of jitter and bias error. The 2-axis gimbal is shown again with the sensor field of view (FOV) and/or divergence projected (solid red lines) as the large tan circular pattern in the figure. The red- cross is the pattern center or instantaneous aim-point. The target location within the sensor field of view is the blue-red square. Perfect tracking is shown in the upper left caption with the red-cross aim-point superimposed on the blue-red target square. The upper right shows the effect of a constant bias error; the aim-point being offset by a constant pointing error. The combination of pointing bias and jitter is then shown superimposed on the sensor FOV in the main figure. The bias offset, shown by the black cross, is the longer term offset error, often due to mounting/component misalignment. Jitter is a short term deviation about a zero mean and it generates a radial jitter envelope shown by the striped gray circle in the figure. The aim-point (red-cross) is offset to the black cross and can lie anywhere within jitter radial envelope. The impact of jitter on pointing depends a lot on the sensor characteristics; primarily instantaneous FOV (IFOV: FOV subtended by a pixel) and frame rate (FR). For geo-location, jitter will manifest itself as increased pointing error reducing geo-location accuracy. Geo-locating an image often uses an image-registration technique (described in Section 4.0). This is a process that compares and aligns a sensed image with a geo-referenced stored image. Severe jitter can result in image blurring. This will reduce the effectiveness of the image processing used to align the sensed image with the referenced image, thereby reducing the overall location accuracy of the geo-registration. For example, frame rate or integration time essentially bounds the camera disturbance frequency spectrum at $F_{DF} = \max(FR, 1/(2*Ti))$. The IFOV can be used to estimate a bound for the worst case angular rate jitter as approximately $|\omega_{dist}| < IFOV * (2\pi * F_{DF})$.

The last topic addressed for the overview is performance. Given all the SLC considerations described how does one evaluate overall performance? Figure 6.0 is a somewhat highly condensed chart describing the overall performance evaluation process. Performance at a system level must

 Copyright© 2019 Peter J. Kennedy

flow down from system or mission requirements. Sensor components are chosen to meet or exceed those requirements. This process is illustrated by the dark brown square centered in the figure. The platform and system component jitter and bias disturbance environment is characterized in an error budget or allocation, conceptually illustrated in the upper right hand corner. Allocation is generally considered the desired distribution of errors while the budget is what evolves with the realities of the actual design. The physical interpretation of the jitter and bias error, discussed previously, is again shown in the upper left corner. An algorithm is then required for evaluating a performance metric as a function of the jitter and bias error. This is often based upon an estimated statistical distributions of jitter and the bias. The example provided in the bottom right side of the figure is termed the Rician Distribution derived from a bi-normal pointing distribution and weighed by a beam shape profile. However the metric should be chosen that best fits the application. The metric shown may work well for LIDAR but geo-pointing with a passive sensor may only require the pointing distribution. Using a metric, the impact of jitter and bias error on performance can be predicted. Initially looking at an uncompensated design to establish the overall level of compensation required followed by introducing the required compensation controls and isolation. For example for the metric described pointing energy on target can be predicted as a function of the jitter and bias error. The plot in the bottom right are constant contours of EOT as a function of normalized jitter and bias error. It can be observed there is a range of jitter and bias values that can meet the desired EOT. Similar plots could be obtained for only pointing probability. Required EOT or pointing probability would be a system performance requirement to meet a mission objective.

Section 1.0 Key Points Summary

- ***SLC two part problem: (i) LOS Track/Point and (ii) LOS stabilization***
- ***Performance defined by sensor requirements (i.e. geo-pointing accuracy) and LOS stability for sensor to meet its requirements over the platform disturbance envelope***
- ***Disturbances to LOS characterized in terms of jitter and bias; quantified by disturbance type in an error budget***
- ***Pointing metric is required to evaluate pointing performance and design tradeoffs to meet performance***

Copyright© 2019 Peter J. Kennedy

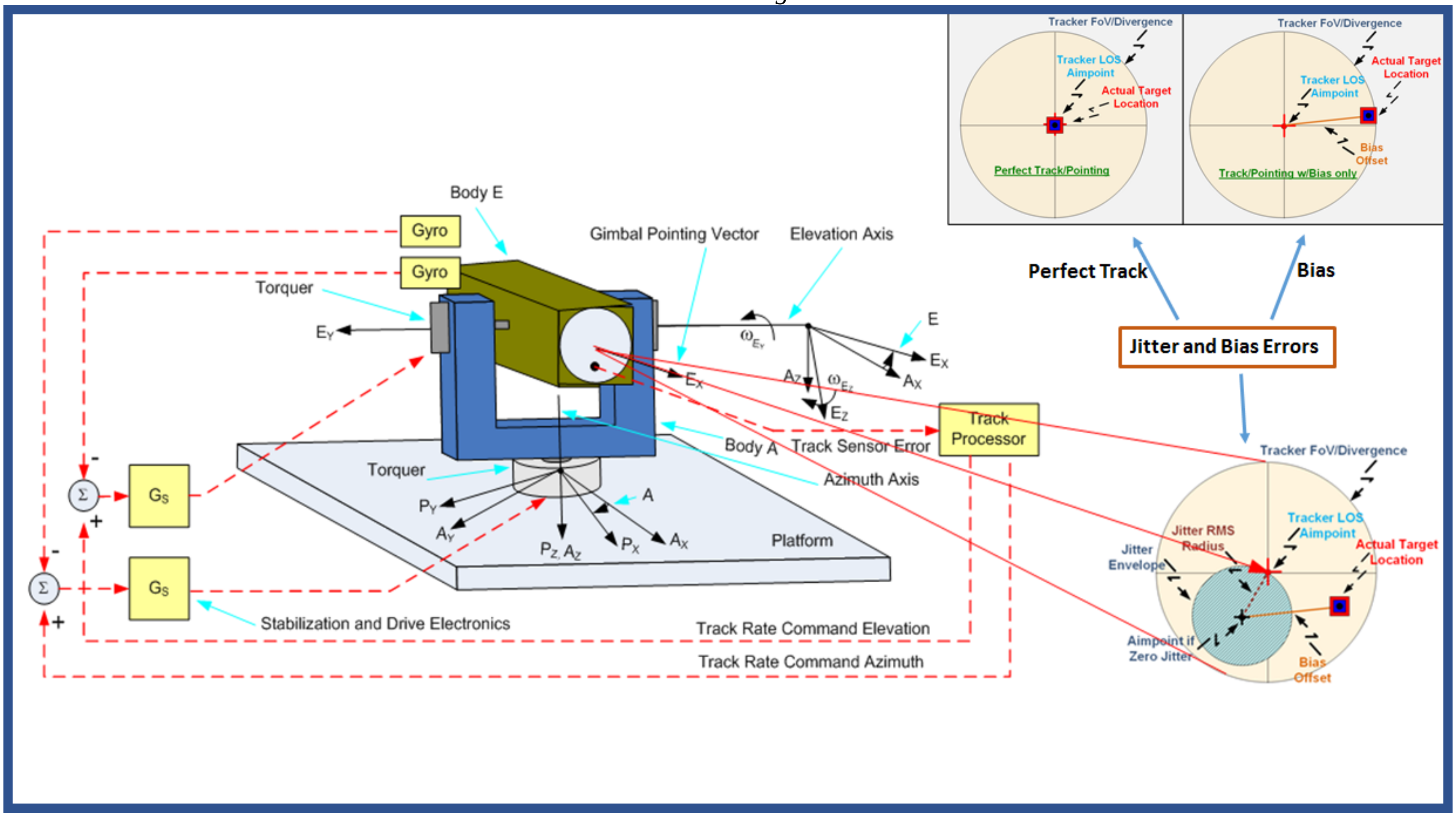

Figure 5.0 Illustration of Jitter and Bias Pointing Error

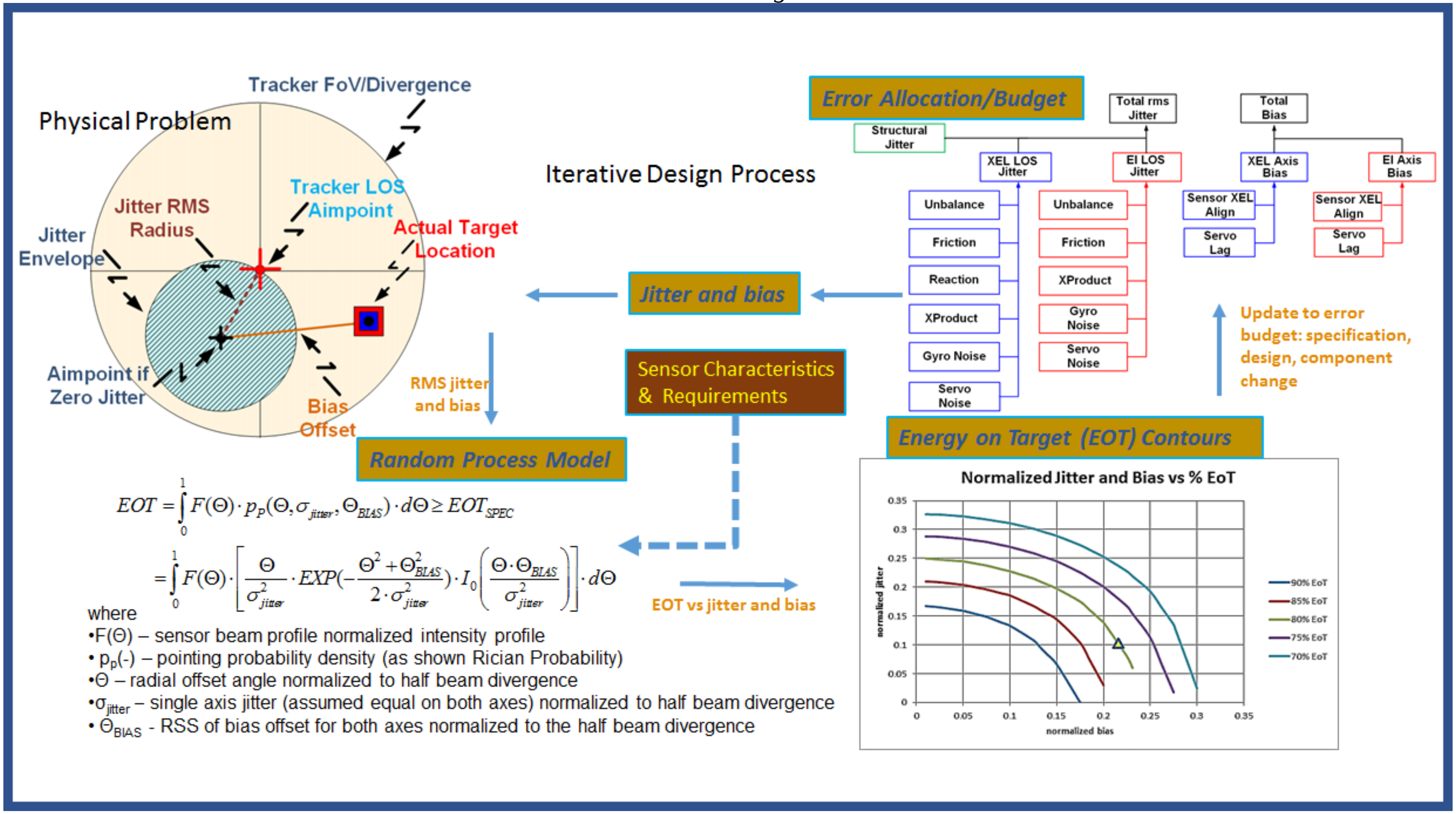

Figure 6.0 SLC Performance Evaluation Process

2.0 SLC Control Architecture [1, 2, 3]

SLC control architectures can be described relative to the gimbal location of the inertial sensors (gyro's or IMU); generally categorized as either direct or indirect stabilization. Direct stabilization refers to the inertial sensors being mounted directly on the LOS axes as shown in the two axis gimbal configuration used in several previous figures. Indirect stabilization implies that the sensors are not mounted on the LOS axes but on an outer axis or the platform gimbal mount. The different configurations are shown in Figure 7.0. A direct SLC architecture (top drawing in figure) is normally recommended for precision pointing applications if at all possible; unfortunately often it is not due to size or weight constraints. The inertial rate sensors are integrated with the body to be stabilized. The coordinate frame attached to the stabilized body is the 'inner rotation axis' or sensor coordinate frame whose X-axis defines the pointing vector. This configuration directly senses disturbance rates orthogonal to the LOS vector; to within the track error. Only these sensors are required for stabilization. The technique is simple to implement, requiring only two angular rate sensors or gyros mounted on the pointing axes and the associated rate loop compensation. With Indirect LOS stabilization (bottom drawing in figure) the rate sensors are mounted on the platform or gimbal outer axes to measure platform motion. It can alleviate some of the problems associated with the direct stabilization design, specifically size and accommodating high slew rates. Three rate sensors are required to accurately measure the platform rates. The inertial measurement unit; a package with three gyros oriented to measure rates about three orthogonal axes, is often used. A coordinate transformation matrix is required to mathematically rotate the platform or outer axis rates into LOS coordinates. The transformation matrix needs gimbal angular position measurements. Resolvers or encoders are used to measure the gimbal angles. When the transformed IMU and gimbal angular rates are summed, the two rate disturbances orthogonal to the LOS can be obtained. The pointing and stabilization servo control configuration for both architectures is shown functionally for a single axis in Figure 8.0. With the direct approach (top drawing in figure) the inner inertial rate loop, whose output is LOS rate (LOSR), attempts to null the LOSR error using high gain compensation. This isolates disturbances from the lower gain outer pointing control loop, effectively rejecting angular disturbances to the pointing vector. The gain of the inner stabilization loop compensation elements is generally much greater than those of the outer position loop. By design, this results in the magnitude of the closed stabilization loop frequency response being near unity over the bandwidth of the position loop response, as defined from a position command in a LOS angle out. The rate sensors will rotate only slightly, relative to an inertial reference, in response to a rate disturbance since they are mounted on the pointing vector and within the negative feedback loop. The amount of motion depends upon the response bandwidth of the loop.

 Copyright© 2019 Peter J. Kennedy

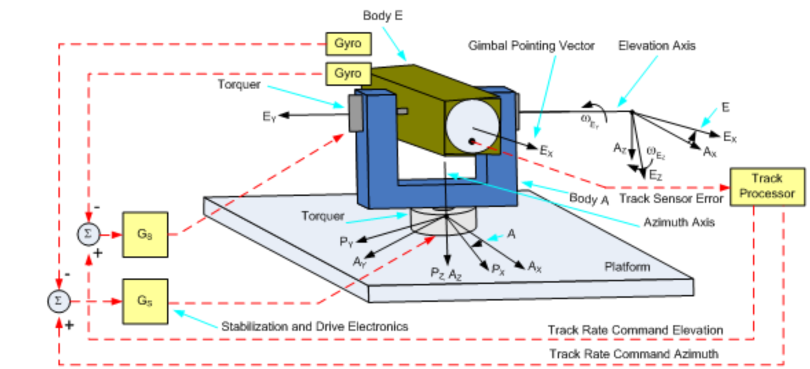

Typical Control Configuration for Direct LOS Stabilization

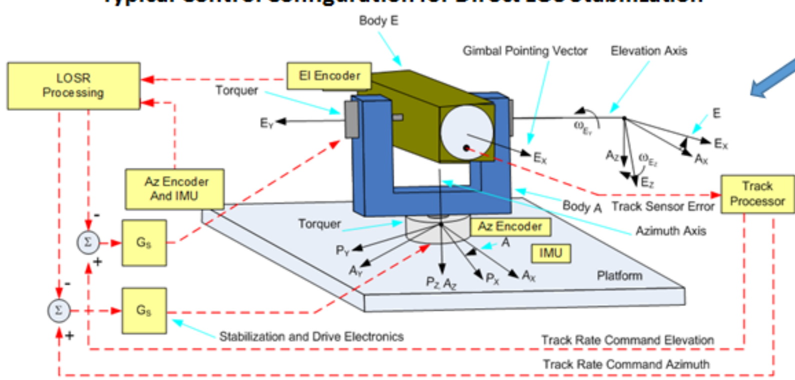

Typical Control Configuration for Indirect LOS Stabilization

- **Direct**
  - **inertial sensors are mounted on the inner most gimbal, axis and/or directly to the stabilized mass whose rotation axes define the LOS coordinates**
- **Indirect platform**
  - **strap-down inertial rate sensors are mounted on the platform measuring platform inertial rates which combined with the gimbal angles are used to derive LOS rates**
- **Indirect outer axis**
  - **inertial rate sensors are mounted on an outer axis measuring inertial rates in outer axis coordinates which combined with the gimbal angles are used to derive LOS rate**

Regardless of approach, always try and reference control to inertial rate quantities

Figure 7.0 SLC Stabilization Architectures

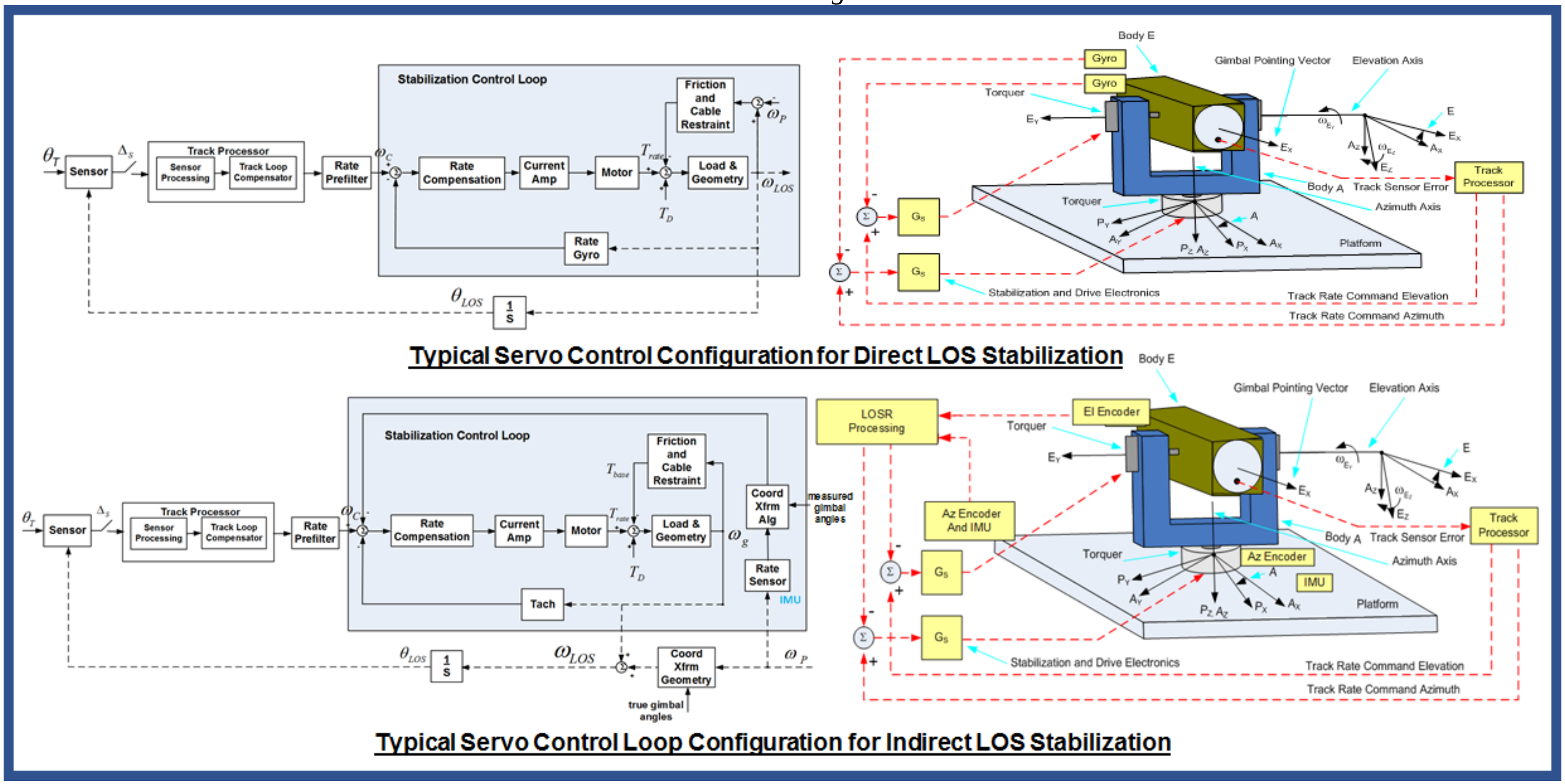

Figure 8.0 SLC Loop Configurations

Copyright© 2019 Peter J. Kennedy

Ideally with infinite bandwidth, they would remain stationary in an inertial reference frame (but rotate relative to the platform). Gimbal size is impacted by the direct approach, since a larger payload volume is required to mount the sensors on the inner axis of the gimbal. For high performance aircraft applications, the penalty in drag and turbulence induced by a large gimbal penetrating the air-stream could be severe. In addition, the sensors must be capable of functioning, or at least withstanding, the high angular rates generated during slew. For the indirect approach (bottom drawing in figure) the platform rates converted to an equivalent rate about the gimbal rotation axis and summed with the gimbal rotation rate relative to its base. It is important to note that in this approach the output of inner rate loop about the stabilized mass is not the inertial rate but the gimbal rate relative to the gimbal base. Disturbances induced by relative motion, such as friction, are compensated by this relative rate feedback loop. The gimbal angular rates are normally measured with either a tachometer or the rate output from a resolver to digital conversion (RDC) circuit card that converts an analog resolver signal to processor digital format. With this approach, the overall accuracy is impacted by scaling, measurement accuracy, differences in processor sampling rate, phase, and processing delays, frequency response differences, and noise associated with the sensor. In addition, the relationship between the actual LOS disturbances and those measured at the base of the gimbal depends upon gimbal geometry and structural rigidity. Indirect and direct stabilization methods differ in that the indirect approach basically requires measurement of the gimbal angles and platform/gimbal rates while the direct method uses the rate sensors and servo loop gain to null the LOS error. Finally the indirect method requires a more complex algorithm and processing than the direct approach. The overview of the SLC stabilization architecture and control configurations provides a basis for now describing the basic theory behind LOS stabilization. Figure 9.0 shows the SLC architecture for a rate loop using the direct approach similar to that in Figure 7.0 in the top drawing. The bottom drawing is a simple mathematical model of this architecture with a generic set of input disturbances. The transfer function between the LOSR -> ω_{LOS} output and the input disturbances and commands (terms covered in light tan overlay) is given by:

$$\omega_{LOS}(s) = \frac{\frac{1}{J \cdot s} \cdot \left(T_D(s) + T_F(s) + \left(B + \frac{K_{CR}}{s} \right) \cdot \omega_P(s) + Ka \cdot Kt \cdot Ks \cdot G_S(s) \cdot \left(\omega_C(s) + \eta(s) \right) \right)}{1 + \frac{1}{J \cdot s} \left(\left(B + \frac{K_{CR}}{s} \right) + Ka \cdot Kt \cdot Ks \cdot G_{GYRO}(s) \cdot G_S(s) \right)}$$

s - LaPlace Transform

Copyright© 2019 Peter J. Kennedy

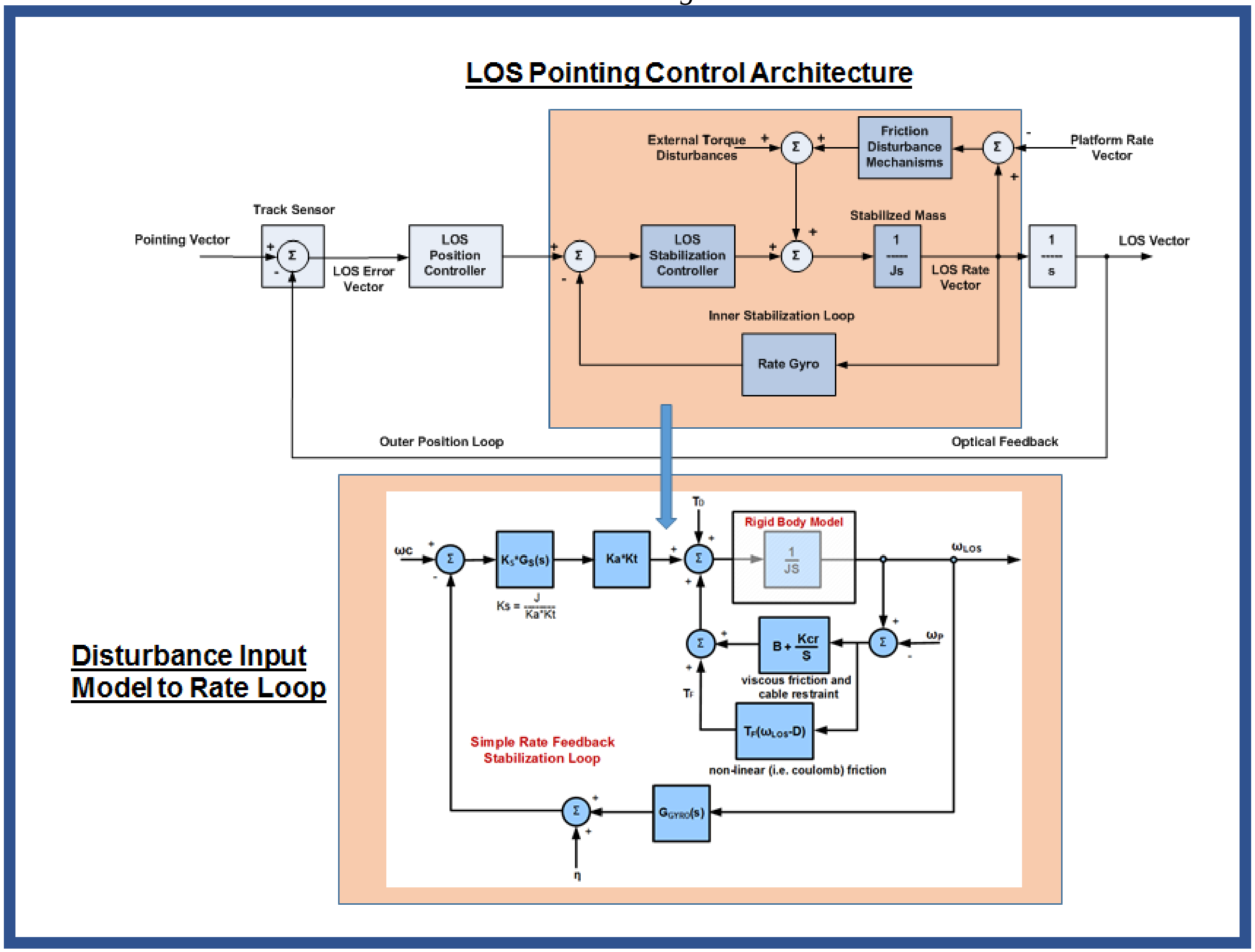

Figure 9.0 SLC Control Configuration and Disturbance Input Model

 Copyright© 2019 Peter J. Kennedy

Key to LOS disturbance rejection is the LOSR feedback; specifically a gain G_S (term covered in light blue overlay) in the feedback loop. To see this, simplify loop so that all inputs except T_D are zero and K_S=J, K_T=K_A=G_{gyro}=1 then solve for ω_{LOS}.

$$\omega_{LOS}(s) = \frac{1}{J \cdot s}\left(T_D + J \cdot G_S(s) \cdot \left(\omega_C(s) - \omega_{LOS}(s)\right)\right) \Rightarrow \omega_{LOS}(s) = \frac{\frac{1}{J \cdot s} \cdot T_D}{1 + \frac{1}{s} \cdot G_S(s)} \quad if \quad \omega_C(s) = 0$$

It can be seen that LOS disturbance rejection is achieved via the rate feedback loop gain, Gs, or approximating the previous equation for high gain:

$$\left|\omega_{LOS}(s)\right| \approx \left|\frac{\frac{T_D}{J}}{G_S(s)}\right| \quad for \quad \left|\frac{1}{s} \cdot G_S(s)\right| >> 1$$

The goal is for ω_{LOS} -> 0; as |Gs|->∞ with disturbances and with a command and $\omega_{LOS} = \omega_C$. The term Gs is really more than simply a gain, but the servo loop compensator consisting of several loop shaping elements; likely PI or PID plus lead/lag elements, notch and roll off filters. Relating this back to Figure 4.0, the LOSR equation is shown again in Figure 10.0 below with key disturbance sources broken out and servo compensation highlighted. Disturbance torques will include several sources, but in general with LOSR feedback disturbance attenuation is obtained from the gain of the compensator G_S; higher the gain, the greater the attenuation. It can also be observed from the last equation that disturbance torques are also weighted by inertia equating to disturbance acceleration; greater inertia lower acceleration disturbance. In effect, Inertia is a friend to stabilization, but not necessarily the size of the torque motor.

Section 2.0 Key Points Summary

- ***Two SLC Stabilization approaches: (i) Direct LOS Stabilization and (ii) Indirect LOS stabilization***
- ***Direct LOS Stabilization Inertial sensors (gyro's or IMU) mounted directly on LOS axis; LOSR sensed directly***
- ***Indirect LOS Stabilization Inertial sensors (gyro's or IMU) mounted on outer axis or gimbal base; LOSR must be calculated***
- ***LOSR feedback key to LOS stabilization design; loop gain proportional to disturbance rejection; greater gain, greater rejection within servo design limits***

 Copyright© 2019 Peter J. Kennedy

$$\omega_{LOS} = \frac{\frac{1}{s}\cdot\left(\frac{T_D}{J}\right)}{1+\frac{1}{J\cdot s}\left(\left(B+\frac{K_{CR}}{s}\right)+Ka\cdot Kt\cdot Ks\cdot G_{GYRO}\cdot G_S(s)\right)} + \quad \rightarrow \text{disturbance torques}$$

$$\frac{\frac{1}{s}\cdot\left(\frac{T_F}{J}+\left(\frac{B}{J}+\frac{K_{CR}}{J\cdot s}\right)\cdot\omega_P(s)\right)}{1+\frac{1}{J\cdot s}\left(\left(B+\frac{K_{CR}}{s}\right)+Ka\cdot Kt\cdot Ks\cdot G_{GYRO}\cdot G_S(s)\right)} + \quad \rightarrow \text{friction and cable restraint torques}$$

$$\frac{\frac{1}{J\cdot s}\cdot\left(Ka\cdot Kt\cdot Ks\cdot G_S(s)\cdot\eta(s)\right)}{1+\frac{1}{J\cdot s}\left(\left(B+\frac{K_{CR}}{s}\right)+Ka\cdot Kt\cdot Ks\cdot G_{GYRO}\cdot G_S(s)\right)} + \quad \rightarrow \text{sensor noise}$$

$$\frac{\frac{1}{J\cdot s}\cdot\left(Ka\cdot Kt\cdot Ks\cdot G_S(s)\cdot\omega_C(s)\right)}{1+\frac{1}{J\cdot s}\left(\left(B+\frac{K_{CR}}{s}\right)+Ka\cdot Kt\cdot Ks\cdot G_{GYRO}\cdot G_S(s)\right)} \quad \rightarrow \text{command rate}$$

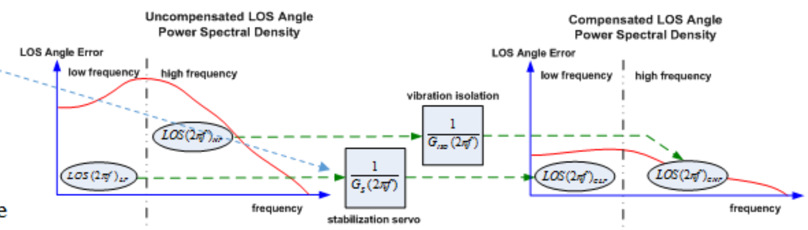

Conceptual Performance of Stabilization and Vibration Isolation

Figure 10.0 SLC LOSR Feedback Equation Mapped back to Disturbance Error

Copyright© 2019 Peter J. Kennedy

3.0 LOS Control of Rigid Body Dynamics [1, 2, 3]

The Rigid Body (RB) dynamics describes the angular motion of a rigid body. The RB Equation (RBE) is a 3 element vector equation providing a mathematical model for the dynamics of the inertial mass for each rotating axis. In the simplest sense; it is the inertia block in a simple control loop block diagram.

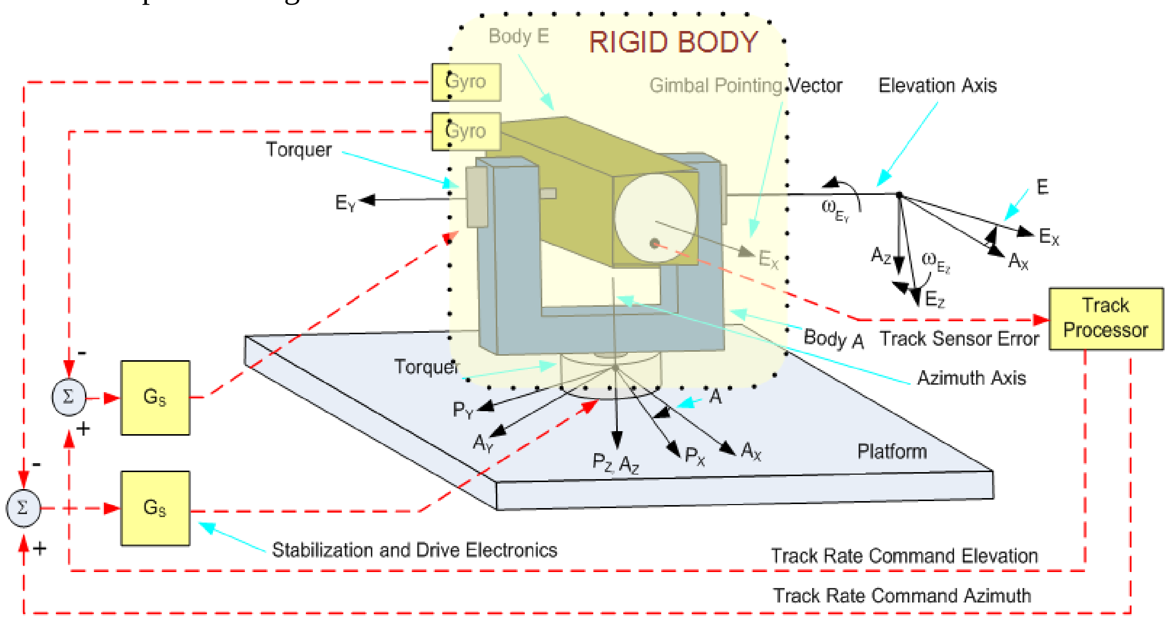

Figure 11.0 the 2-Axis Gimbal Configuration Highlighting Rigid Body Elements

The highlighted portion of the figure is the Rigid Body; effectively the gimbal mounted to the platform; although not necessarily rigid it is treated as such. Structural flexure is normally addressed separately via mechanical finite element analysis (FEA). For a gimbal with multiple axes and rotating inertias the Rigid Body Model (RBM) describes the composite dynamics for all axes whose characterization is critical to the LOS Control design. There is a 3-D inertial coordinate frame associated with each gimbal rotation stage for which the RBE defines the axis inertial mass dynamics (note in inertial coordinates even a non-rotating gimbal axis can have motion about it). Gimbal rotation stages are normally defined from inner to outer as:

- inner being the final LOS control stage on which the sensor or a steering mirror interfacing optically to the sensor is mounted.
- outer most stage is mounted to the platform

It is important to keep in mind the overall objective is to control the LOS axes; albeit via the gimbal rotation axes. The vector equation that describes the angular rate and acceleration dynamics of a rigid body derived from equating the sum of the kinematic torques applied to a rigid body to its

 Copyright© 2019 Peter J. Kennedy

rate of change of angular momentum. They are often termed Euler's Rigid Body Equations for whom originally derived them from:

$$\hat{L}(t) = \frac{d\hat{H}(t)}{dt}$$

$\hat{L}(t)$ – vector sum of torques applied to body ; $\hat{H}(t)$ – angular momentum of body

For each rotating gimbal axis there is an associated mass rotating in its 3-D coordinate frame; this is the rigid body for that rotating axis. The RBE describes the rate and acceleration dynamics of the body about each axis of the coordinate frame in an inertial reference. One axis is controlled and includes the motor torques and torque disturbances in the torque summation for that axis while and the other two axes generate reaction torques applied to the next outer most rotating stage. The full momentum equation includes many torque terms including offsets between rotation center and center of mass for each rigid body as well as differences in rotation centers between rigid body axes coordinate frames. However if there are no offsets then the momentum expression reduces to:

$$\hat{H}(t) = \overline{J} \cdot \hat{\omega} \quad \text{where } \overline{\mathrm{J}} \text{ is the inertia matrix given by:}$$

$$\overline{J} = \begin{bmatrix} J_{xx} & J_{xy} & J_{xz} \\ J_{yx} & J_{yy} & J_{yz} \\ J_{zx} & J_{zy} & J_{zz} \end{bmatrix}$$

Differentiation of the momentum vector results in the basic Rigid Body Vector Equation:

$$\frac{d\hat{H}(t)}{dt} = \overline{J} \cdot \dot{\hat{\omega}} + \hat{\omega} \times \overline{J} \cdot \hat{\omega}$$

$$or \qquad \hat{L}(t) = \overline{J} \cdot \dot{\hat{\omega}} + \hat{\omega} \times \overline{J} \cdot \hat{\omega}$$

Expanding this expression, angular rates and accelerations are related to a torque summation (L_X, L_Y, L_Z) for each axis as:

$$L_X = J_{XX}\dot{\omega}_X + (\dot{\omega}_Y - \omega_X\omega_Z)J_{XY} + (\dot{\omega}_Z + \omega_X\omega_Y)J_{XZ} + (J_{ZZ} - J_{YY})\omega_Y\omega_Z + (\omega_Y^2 - \omega_Z^2)J_{YZ}$$
$$L_Y = J_{YY}\dot{\omega}_Y + (\dot{\omega}_X + \omega_Y\omega_Z)J_{YX} + (\dot{\omega}_Z - \omega_X\omega_Y)J_{YZ} + (J_{XX} - J_{ZZ})\omega_Z\omega_X + (\omega_Z^2 - \omega_X^2)J_{ZX}$$
$$L_Z = J_{ZZ}\dot{\omega}_Z + (\dot{\omega}_X - \omega_Y\omega_Z)J_{ZX} + (\dot{\omega}_Y + \omega_X\omega_Z)J_{ZY} + (J_{YY} - J_{XX})\omega_Y\omega_X + (\omega_X^2 - \omega_Y^2)J_{XY}$$

For each axis this set of three equations will have one for a rotating axis and the other two constrained by the axis bearing producing reaction torques in inertial space on the next outer most rigid body structure that supports the rotating axis bearing and shaft. For the rotating axis, the torque summation is the driving input consisting of a control and disturbance torques. For the non-rotating or gimbal constrained axes, the torques are outputs, as calculated from the angular rates

 Copyright© 2019 Peter J. Kennedy

and accelerations to the right, applied through the rotating axis bearing producing reaction torques in inertial space on the next outer most rotating stage of the rigid body structure supporting the rotating axis bearing and shaft. The off-axis terms (xy, xz, yz) can be considered dynamic imbalance torques. If the inertia cross products are zero (i.e. $J_{XY}=J_{YZ}=J_{XZ}=0$), then only the principle axis inertias remain and the equation reduces to:

$$L_X = J_{XX}\dot{\omega}_X + (J_{ZZ} - J_{YY})\omega_Y\omega_Z$$
$$L_Y = J_{YY}\dot{\omega}_Y + (J_{XX} - J_{ZZ})\omega_Z\omega_X$$
$$L_Z = J_{ZZ}\dot{\omega}_Z + (J_{YY} - J_{XX})\omega_Y\omega_X$$

The reaction torques, discussed previously, although part of torque summation are often broken out as an explicit quantity since they will impact several terms in the RBE including the effective inertia referenced to the LOS. The torque equation for axis N can be expressed as:

$$\hat{L}_N(t) = \overline{J}_N\dot{\hat{\omega}}_N(t) + \hat{\omega}_N(t)\times\overline{J}_N\hat{\omega}_N(t) - (\hat{L}_{N-1}(t))_N \quad \text{'}\times\text{'-denotes cross-product}$$

or since $(\hat{L}_{N-1}(t))_N = \overline{R}^T_{N-1}\cdot\hat{L}'_{N-1}(t)$ $\quad\hat{L}'_{N-1}(t)$ – axis N-1 off-axis torque vector

$$\hat{L}_N(t) = \overline{J}_N\dot{\hat{\omega}}_N(t) + \hat{\omega}_N(t)\times\overline{J}_N\hat{\omega}_N(t) - \overline{R}^T_{N-1}\cdot\hat{L}'_{N-1}(t)$$

The reaction torque applied to axis N is shown rotated into the gimbal coordinate frame for axis N via the inverse of coordinate frame N-1's rotation matrix. For the inner most rotation axis; the reaction torque term is zero since being the most inner axis there are reaction torques being applied to it from a more inner axis. While Rigid Body motion describes inertial rate and acceleration for the body coordinate frame rotating axis; inertial rate and acceleration kinematics for gimbal non-rotating axes are obtained by rotating a rate vector (usually starting with platform rate) through one coordinate frame to the next. Angular rate and acceleration vectors between coordinate frames, going outer (N+1) to inner (N), are obtained from then following kinematic equations with the exception of the rotating axis component; as derived from the Rigid Body Dynamics discussed previously.

$$\text{angular rate:} \qquad \hat{\omega}_N(t) = \begin{bmatrix}\omega_{NX}(t)\\ \omega_{NY}(t)\\ \omega_{NZ}(t)\end{bmatrix} = \overline{R}_N(t)\cdot\hat{\omega}_{N+1}(t) + \dot{\hat{N}}(t)$$

$$\text{angular acceleration:} \quad \dot{\hat{\omega}}_N(t) = \overline{R}_N(t)\cdot\dot{\hat{\omega}}_{N+1}(t) + \hat{\omega}_{N+1}(t)\times\dot{\hat{N}}(t) + \ddot{\hat{N}}(t)$$

$\overline{R}_N(t)$ - rotation matrix for axis N ; 'x' - vector cross product

$\dot{\text{N}}$(t) - axis N coordinate frame relatve rate with respect to axis N + 1 coordinate frame

Copyright© 2019 Peter J. Kennedy

For example roll (r) rotates about the x-axis, elevation (E) about the y'-axis, azimuth (A) about the z''-axis where the prime denotes that axis after prior rotation. The rotation angles are termed the Euler angles and the rotation matrices are given by:

$$\bar{R}_r(t)=\begin{bmatrix}1 & 0 & 0\\ 0 & c_r(t) & s_r(t)\\ 0 & -s_r(t) & c_r(t)\end{bmatrix};\quad \bar{R}_E(t)=\begin{bmatrix}c_E(t) & 0 & -s_E(t)\\ 0 & 1 & 0\\ s_E(t) & 0 & c_E(t)\end{bmatrix};\quad \bar{R}_A(t)=\begin{bmatrix}c_A(t) & s_A(t) & 0\\ -s_A(t) & c_A(t) & 0\\ 0 & 0 & 1\end{bmatrix}$$

$$c_x(t)=\cos(x(t)) \quad , \quad s_x(t)=\sin(x(t))$$

The rotation matrices discussed can be multiplied in an ordered sequence (i.e. outer starting at platform to inner) providing the orientation of one coordinate frame to another as generated by several rotations. This matrix product, termed the direction cosine matrix (DCM), defines the orientation between the two coordinate frames (i.e. platform or inertial and the inner axis or LOS coordinates) or:

$$D\bar{C}M_{N+m}^{N}(t)=\bar{R}_N(t)\cdot\bar{R}_{N+1}(t)\cdot \;.....\; \cdot\bar{R}_{N+m-1}(t)\cdot\bar{R}_{N+m}(t)$$

It is termed the direction cosine matrix since the elements define the cosine of the angle between the x, y, z axes of coordinate frame 1 and coordinate frame 2. For example element 1, 1, would be cos(x1, x2) and element 1, 2 cos(x1, y2) etc. The DCM plays a critical role in deriving the LOS and LOSR vectors. LOS control also requires an algorithm to project a target inertial vector into LOS coordinates. The rotation matrices describe the orientation between inertial and LOS coordinates. This rotation matrices sequence structure becomes the basis for defining LOS and LOSR vectors. A generic target vector is defined in inertial coordinates for some azimuth angle, A_T, and elevation angle, E_T. Often the x-axis is defined as the pointing axis so the target vector is given as:

$$\hat{P}_{TGTI}=\bar{R}^T(A_T)\cdot\bar{R}^T(E_T)\cdot\begin{bmatrix}1\\0\\0\end{bmatrix}=\begin{bmatrix}c_{A_T}(t) & -s_{A_T}(t) & 0\\ s_{A_T}(t) & c_{A_T}(t) & 0\\ 0 & 0 & 1\end{bmatrix}\cdot\begin{bmatrix}c_{E_T}(t) & 0 & s_{E_T}(t)\\ 0 & 1 & 0\\ -s_{E_T}(t) & 0 & c_{E_T}(t)\end{bmatrix}\cdot\begin{bmatrix}1\\0\\0\end{bmatrix}=\begin{bmatrix}c_{A_T}(t)\cdot c_{E_T}(t)\\ s_{A_T}(t)\cdot c_{E_T}(t)\\ -s_{E_T}(t)\end{bmatrix}$$

A geometric interpretation of the target vector is shown below in Figure 12.0.

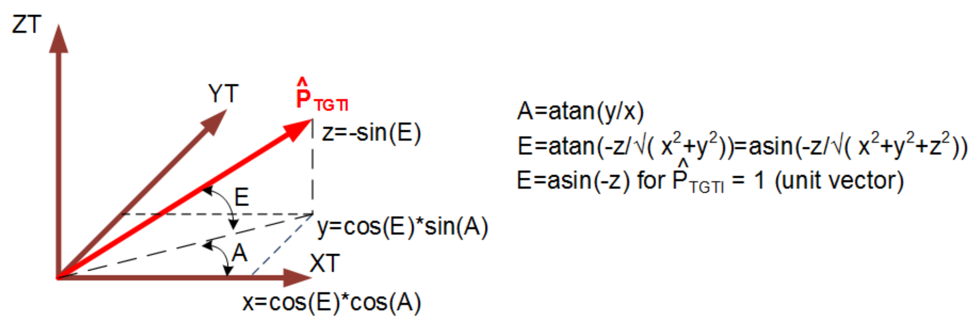

Figure 12.0 General Pointing Vector

Copyright© 2019 Peter J. Kennedy

The target vector must be rotated from inertial to LOS coordinates. The platform DCM follows the matrix sequence for platform roll (R), pitch (P), and yaw (Y) given as (El-> pitch, Azimuth->yaw):

$$D\bar{C}M_I^P = \bar{R}(roll_P)\cdot\bar{R}(pitch_P)\cdot\bar{R}(yaw_P)$$

The inertial target vector rotates into platform coordinates as:

$$\hat{P}_{TGTP} = D\bar{C}M_I^P \cdot \hat{P}_{TGTI}$$

With the simple 2-axis design, discussed in previous sections, the inner axes are the LOS axes so rotating the target vector through the DCMs into the inner coordinate frame provides the LOS vector from which the LOS angles can be determined.

$\hat{P}_{TGTLOS} = \bar{R}_E \cdot \bar{R}_A \cdot \hat{P}_{TGTP}$ target vector in platform coordinates rotated into inner gimbal LOS coordinates

$\hat{P}_{TGTLOS} = \bar{R}_E \cdot \bar{R}_A \cdot D\bar{C}M_I^P \cdot \hat{P}_{TGTI}$

$\hat{P}_{TGTLOS} = D\bar{C}M_P^E \cdot D\bar{C}M_I^P \cdot \hat{P}_{TGTI} = D\bar{C}M_I^E \cdot \hat{P}_{TGTI}$

where $D\bar{C}M_P^E = \bar{R}_E \cdot \bar{R}_A$ and $D\bar{C}M_I^E = D\bar{C}M_P^E \cdot D\bar{C}M_I^P$

But since $D\bar{C}M_I^{LOS} = D\bar{C}M_I^E$ (E -> LOS) a <u>key pointing relationship</u> can be expressed as the product of the two DCMs; inertial->platform; platform->LOS or:

$$D\bar{C}M_I^{LOS} = D\bar{C}M_P^{LOS} \cdot D\bar{C}M_I^P$$

LOS<-inertial ~ LOS<-platform; platform<-inertial

The LOS angles can be determined from the geometry example provided on the last slide or by simply noting it is desired: $\hat{P}^T_{TGTLOS} = \begin{bmatrix}1 & 0 & 0\end{bmatrix}$. The LOS angles satisfying this criterion can be determined from the target platform vector by meeting the condition:

$$\hat{P}_{TGTP} = \bar{R}_A^T \cdot \bar{R}_E^T \cdot \begin{bmatrix}1\\0\\0\end{bmatrix} = \begin{bmatrix}c_A \cdot c_E\\ s_A \cdot c_E\\ -s_E\end{bmatrix}$$

$$\text{perfect pointing is obtained if : } A = \text{atan}\left(\frac{P_{TGTPY}}{P_{TGTPX}}\right);\ E = \text{atan}\left(\frac{-P_{TGTPZ}}{\sqrt{P_{TGTPX} + P_{TGTPY}}}\right)$$

In general, the control algorithm will not produce the exact angles, the vector zero components will be errors or: $\hat{P}^T_{TGTLOS} = \begin{bmatrix}1 & e_{AZ} & e_{EL}\end{bmatrix}$. The last two vector components are azimuth and elevation LOS pointing errors. A pointing example using DCMs, more pertinent to a geo-pointing application is locating another geographical location or target from a remote platform. With geo-

Copyright© 2019 Peter J. Kennedy

pointing, vector position is generally defined in earth centered earth fixed coordinates (ECEF). A general expression for determining a target location from a remote location is given by the sum of the platform position in ECEF coordinates plus the calculated relative target vector for measured range as:

$$\hat{P}_{TGT}^{ECEF} = \hat{P}_{PLAT}^{ECEF} + range \cdot D\bar{C}M_{LOS}^{ECEF} \begin{bmatrix} 1 \\ 0 \\ 0 \end{bmatrix}$$

where :

$$D\bar{C}M_{LOS}^{ECEF} = D\bar{C}M_{NED}^{ECEF} \cdot D\bar{C}M_{PLAT}^{NED} \cdot D\bar{C}M_{GIMBAL}^{PLAT} \cdot D\bar{C}M_{LOS}^{GIMBAL} \text{ - } DCM\ \ LOS\ to\ ECEF$$

$$D\bar{C}M_{NED}^{ECEF} \text{ - } DCM\ \ NED\ to\ ECEF\ (earth\ centered\ earth\ \ fixed)$$

$$D\bar{C}M_{PLAT}^{NED} \text{ - } DCM\ \ Platform\ to\ North\ East\ Down\ (NED)$$

$$D\bar{C}M_{GIMBAL}^{PLAT} \text{ - } DCM\ \ Gimbal\ \ to\ \ Platform$$

$$D\bar{C}M_{LOS}^{GIMBAL} - DCM\ \ LOS\ to\ Gimbal\ \ \ (i.e.\ sensor)$$

The geo-pointing problem will be discussed in more detail in Section 8.0 along with the definition of the associated coordinate frames used with geo-pointing. The north east down (NED) frame in this equation is really the inertial coordinate frame defined as the inertial reference throughout the first sections of the course. Platform position in ECEF Cartesian coordinates is obtained from the platform GPS; platform geodetic latitude (WGS84), Φ, longitude (WGS84), Λ, and altitude as:

$$\hat{P}_{PLAT}^{ECEF} = \begin{bmatrix} \left(\dfrac{R_{EQ}}{\sqrt{1-e^2 \cdot \sin^2(\Phi)}} + \text{altitude} \right) \cdot \cos(\Phi) \cdot \cos(\Lambda) \\ \left(\dfrac{R_{EQ}}{\sqrt{1-e^2 \cdot \sin^2(\Phi)}} + \text{altitude} \right) \cdot \cos(\Phi) \cdot \sin(\Lambda) \\ -\left(\left(\dfrac{R_{PL}}{R_{EQ}} \right)^2 \cdot \dfrac{R_{EQ}}{\sqrt{1-e^2 \cdot \sin^2(\Phi)}} + \text{altitude} \right) \cdot \sin(\Phi) \end{bmatrix}$$

Where the earth's semi-major axis R_{EQ} = 20, 925, 646 feet (earth's radius at equator), R_{PL}=20, 850, 147.59 (earths radius at pole) and the square of the earth's eccentricity e^2 = 0.00669438. The relationship between geodetic latitude measured by the GPS and geocentric latitude is:

$$\tan(\Phi_{geocentric}) = \left(\frac{R_{PL}}{R_{EQ}} \right)^2 \cdot \tan(\Phi)$$

The DCMs in the equation are determined from the platform longitude, geodetic latitude, inertial navigation system (INS) measured platform angles, and gimbal azimuth and elevation angles. Perfect pointing is assumed, more likely a track sensor will be pointing the gimbal so there would

 Copyright© 2019 Peter J. Kennedy

be associated track error terms replacing the zeroes in the LOS pointing vector. Again this will all be discussed in Section 8.0 and Part 2.

Section 3.0 Key Points Summary

- ***Rigid Body equations were introduced which define the angular motion of the gimbaled pointing structure and LOS dynamics***
- ***Coordinate frame rotations define the orientation of a vector in the coordinate frame attached to each rotating gimbal mass and ultimately the LOS***
- ***A direction cosine matrix (DCM) is a sequence of rotation matrices defining a vector orientation between the initial and end coordinate frame.***
- ***The DCM is a key to describing the orientation of a pointing vector i.e. geo-pointing***
- ***It will be sown it is also a key to deriving the LOSR consistent with the pointing DCM***

4.0 LOS Control 2-Axis Gimbal Example [1, 2, 3]

As an example, the general expression for the RBE discussed in the last section is applied to the 2-axis gimbal design with an optical sensor payload (i.e. camera), on-axis gyros for direct stabilization, and an INS mounted near the gimbal base. The gimbal configuration is the 2-axis gimbal drawing shown in previous figures. Only the principle axis inertias (assume off-axis are zero) are used to keep things simple. In general, there are 3 equations for the elevation axis and 3 equations for the azimuth axis. Assume reaction torques from the azimuth axis to the platform base are not an issue (i.e. large platform), so that for azimuth one only needs the rotation axis or z-axis equation. The gyros mounted on the elevation body will sense $\omega_{LOSY} = \omega_{EY}$ and $\omega_{LOSZ} = \omega_{EZ}$. The general operation is a platform in motion provided with an inertial position that it needs to point to, acquiring an object within the optical sensor field of view (FoV). So one we must consider the LOS stabilization design, the pointing control loop design, and the inertial pointing algorithm. Once there is handoff from pointing control to the optical sensor, it is assumed the track algorithm and track servo loop will do the rest. The rigid body model is described followed by block diagrams of the rate control loop and then the overall pointing control loop architecture. It is important to note that the rigid body equations provide a means of designing the required servo controllers; however they are not necessarily part of the control loop algorithm unless a gimbal model is required; as for an adaptive control application. The RB equations are summarized in Figure 13.0, elevation body RBE in the top half of the figure and the azimuth body RBE in the bottom half. The equations highlighted in orange are for the rotation axis and the blue square denotes the control torque terms generated by the servo controller for each axis. The RBE for both axes are expanded as shown in Figure 14. This diagram is parameterized in terms of only inertial LOS rate and

Copyright© 2019 Peter J. Kennedy

acceleration as outputs and inertial platform rates, acceleration, and torque disturbances as inputs. Although this representation appears much more imposing; it contains a great deal of information showing the inter-relationships between the LOS and the elevation and cross elevation axes. Much of the complexity arises from the reaction torque feedback term input to the azimuth axis, highlighted in tan in Figure 13.0. At the bottom of the block diagram in Figure 14.0 is an expression for the equivalent inertia referenced to the cross elevation LOS axis; showing this inertia is not simply the azimuth inertia but dependent on the elevation axis inertias and elevation angle geometry; which must be accounted for in the servo controller design. Referring to the previous section description using LOSR feedback for control, simple expressions can be obtained for the torque control terms with the basic feedback control architecture for each axis is shown in Figure 15.0. Elevation LOSR feedback is shown on the top and cross elevation LOSR feedback on the bottom loop. Elevation control directly follows the previous discussion. Cross elevation must be obtained by measuring this rate but is implemented indirectly via the azimuth axis and therefore it is divided by the elevation angle cosine to obtain an equivalent azimuth command. Substituting into the expression relating azimuth and cross elevation rates, an additional disturbance term is observed, introduced due to the indirect control of cross elevation via the azimuth rotation axis. Applying the servo feedback control, a block diagram of the basic rate feedback control loop implementation is shown in Figure 16.0 with the individual RBE blocks for each body axis highlighted. Remember these blocks are physical not algorithmic; effectively the body inertias. The rate stabilization servo loop is implemented about the rigid body dynamics with gyros mounted on elevation body directly measuring LOSR. A secant gain in cross elevation converts to the azimuth drive command however if operation is at low elevation angles it may not be needed. To obtain the non-rotating axis angular rates, the kinematic equations for the 2-axis gimbal are required, as described in Section 3.0, with the final expression for the rate transformations from platform to elevation coordinates expressed as:

$$\hat{\omega}_E(t) = \overline{R}_E(t) \cdot \overline{R}_A(t) \cdot \hat{\omega}_P(t) + \overline{R}_E(t) \cdot \hat{\dot{A}}(t) + \hat{\dot{E}}(t)$$

Gimbal inertial and relative rates for the rotating axes are measured while the non-rotating axis rates derived via the kinematic equations. This expression is broken down per axis in Figure 17.0 which also includes angular acceleration descriptions. Finally there is the pointing problem to address which is effectively geo-pointing. The geo-pointing problem was touched upon in Section 3.0, is defined in some detail in Section 8.0; and described in much detail in Part 2 of the course. As such, some simple assumptions will be made to derive pointing angles so an overall architecture can be generated without requiring the details of generating the geo-pointing vector described later.

 Copyright© 2019 Peter J. Kennedy

- **Elevation Axis Vector RBE:**

$$\hat{L}_E(t) = \bar{J}_E\,\dot{\hat{\omega}}_E(t) + \hat{\omega}_E(t) \times \bar{J}_E\,\hat{\omega}_E(t) \quad \text{el-axis vector equation}$$

- **Elevation Axis RBE Elements; y-rotating axis; x,z-reaction torques (*blue square denotes control torque*)**

$$L_{EX} = J_{EX}\dot{\omega}_{EX} + \omega_{LOSY}\,\omega_{LOSZ}\,(J_{EZ} - J_{EY})$$

$$J_{EY}\,\dot{\omega}_{LOSY} = -\omega_{LOSZ}\,\omega_{EX}\,(J_{EX} - J_{EZ}) + \boxed{T_{EY}} - T_{UEY} - T_{EFC}(t)$$

$$L_{EZ} = J_{EZ}\,\dot{\omega}_{LOSZ} + \omega_{EX}\,\omega_{LOSY}\,(J_{EY} - J_{EX})$$

$L_{EX}(t)$, $L_{EZ}(t)$ - reaction torques exerted by inner gimbal on outer gimbal

$L_{EY}(t) = -T_{UEY}(t) + T_{EY}(t) - T_{EFC}(t)$

$T_{UEY}(t)$ - mass imbalance torque

$\boxed{T_{EY}(t)}$ - elevation control torque ; E - gimbal elevation angle

B_{FY} - viscous friction coefficient ; K_{CRY} - cable restraint coefficient

T_{FY}, T_{CRY} - non-linear friction and cable restraint torques

$T_{EFC}(t) = B_{FY}\cdot\dot{E}(t) + K_{CRY}\cdot E(t) + T_{FY}(\dot{E}) + T_{CRY}(E)$

- **Azimuth Axis Vector RBE:**

$$\hat{L}_A(t) = \bar{J}_A\,\dot{\hat{\omega}}_A(t) + \hat{\omega}_A(t) \times \bar{J}_A\,\hat{\omega}_A(t) - (\hat{L}_E(t))_A \quad ; \quad (\hat{L}_E(t))_A = \bar{R}_E^T \cdot \begin{bmatrix} L_{EX} \\ 0 \\ L_{EZ} \end{bmatrix}$$

reaction torque: el -> az

- **Expanding this equation, the vector rotating axis z-component is:**

$$J_{AZ}\dot{\omega}_{AZ} = -\omega_{AY}\,\omega_{AX}\,(J_{AY} - J_{AX}) - L_{EZ}\cdot\cos(E) + L_{EX}\cdot\sin(E) + \boxed{T_{AZ}} - T_{UAZ} - T_{AFC}(t)$$

$L_{AZ}(t) = T_{AZ}(t) - T_{UAZ}(t) - T_{AFC}(t)$

$T_{UAZ}(t)$ - outer gimbal mass unbalance torques;

B_{FZ} - viscous friction coefficient ; K_{CRZ} - cable restraint coefficient

$\boxed{T_{AZ}(t)}$ - control torque; A - gimbal azimuth angle

T_{FZ}, T_{CRZ} - non-linear friction and cable restraint torques

$T_{AFC}(t) = B_{FZ}\cdot\dot{A}(t) + K_{CRZ}\cdot A(t) + T_{FZ}(\dot{A}) + T_{CRZ}(A)$

Figure 13.0 2-Axis Gimbal Rigid Body Model

Copyright© 2019 Peter J. Kennedy

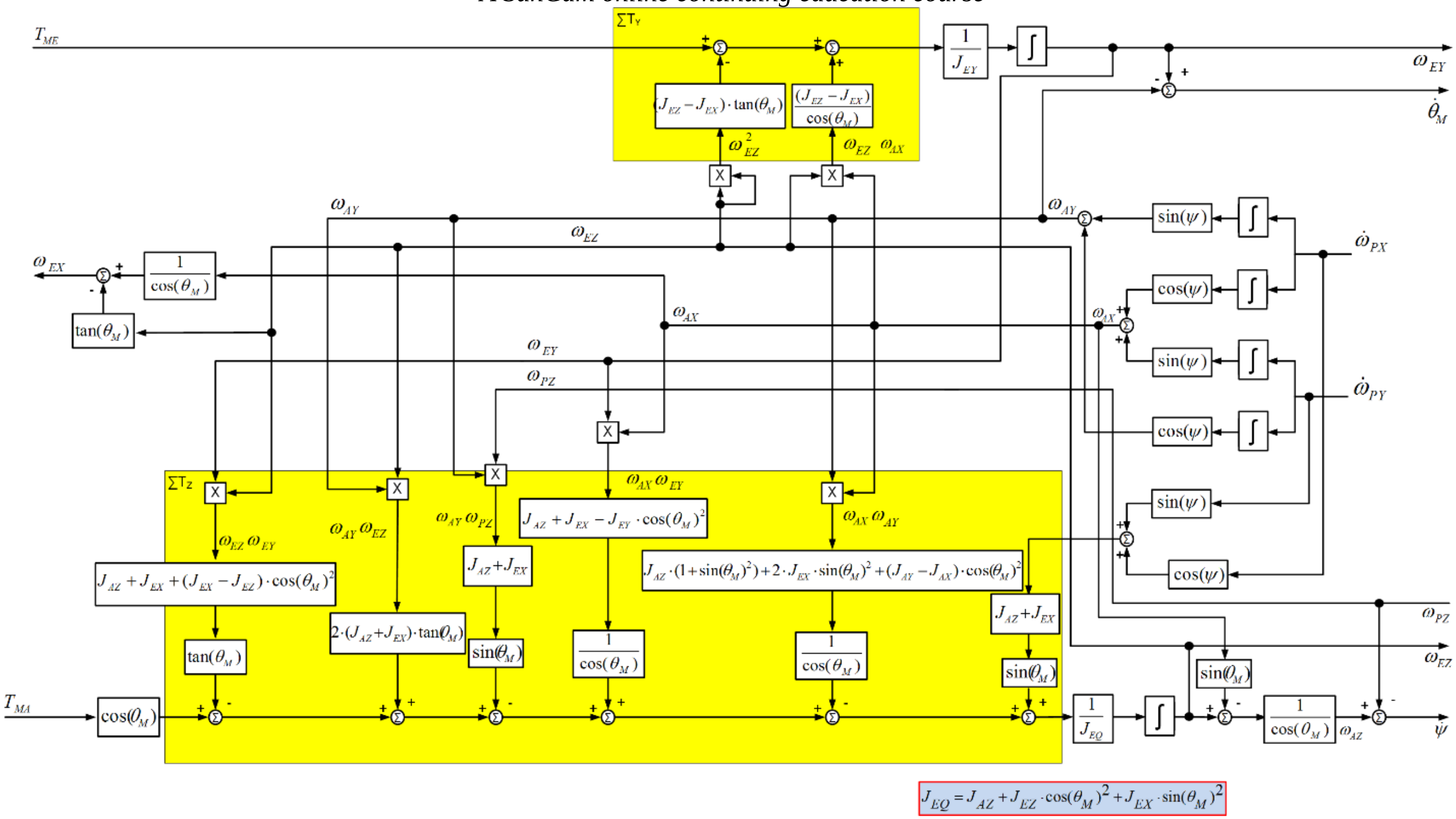

Figure 14.0 Two -Axis RBE Block Diagram

 Copyright© 2019 Peter J. Kennedy

LOS Stabilization: LOSR Feedback Control for Disturbance Rejection

Elevation LOSR Feedback

$\omega_{LOSY} = \omega_{EY}$

El Control Torque

$$T_{EY} = -G_S \cdot \omega_{LOSY} \quad \therefore \quad \omega_{LOSY} = \frac{\frac{1}{J_{EY} \cdot s} \cdot \text{disturbances}}{1 + \frac{1}{J_{EY} \cdot s} \cdot G_S}$$

feedback attenuation; zero command

Cross Elevation LOSR Feedback

$\omega_{LOSZ} = \omega_{EZ}$

Very simplified; formal derivation more complex with effective LOS XEl inertia a composite term not simply Az inertia

Az Control Torque

$$T_{AZ} = -G_S \cdot \frac{\omega_{EZ}}{c_E} \quad \therefore \quad \omega_{AZ} = \frac{1}{J_{AZ} \cdot s}\left(-G_S \cdot \frac{\omega_{EZ}}{c_E} + \text{az disturbances}\right)$$

$$\omega_{EZ} = c_E \cdot \omega_{AZ} + s_E \cdot \omega_{AX} = c_E \cdot \frac{1}{J_{AZ} \cdot s} \cdot \left(-G_S \cdot \frac{\omega_{EZ}}{c_E} + \text{az disturbances}\right) + s_E \cdot \omega_{AX}$$

$$\omega_{EZ} = \frac{1}{1 + \frac{1}{J_{AZ} \cdot s} \cdot G_S} \cdot \left(\frac{c_E}{J_{AZ} \cdot s} \cdot \text{az disturbances} + s_E \cdot \omega_{AX}\right)$$

feedback attenuation; zero command

Figure 15.0 Two-Axis Gimbal LOS Rate Feedback Control Algorithm

Copyright© 2019 Peter J. Kennedy

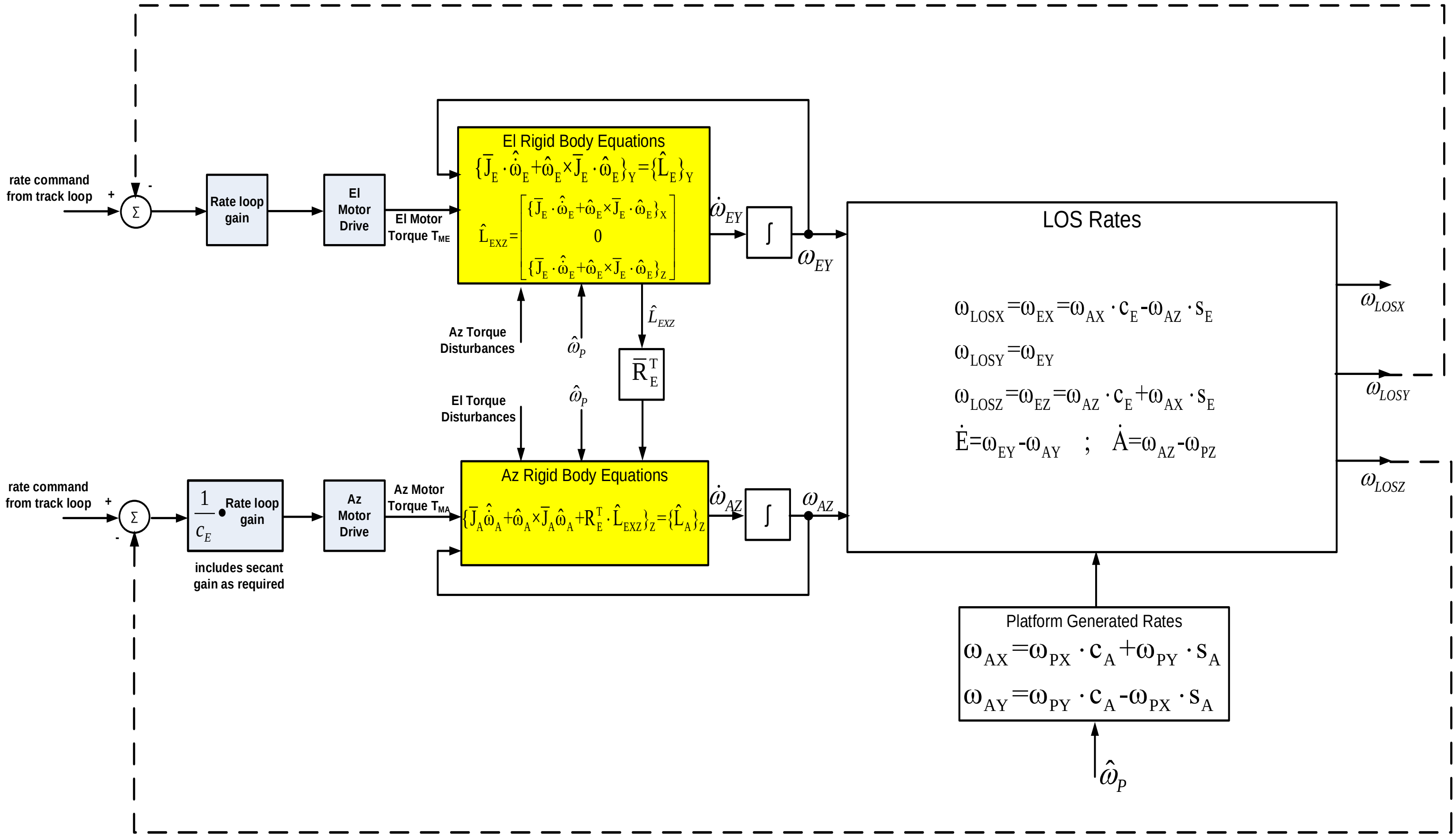

Figure 16.0 Two -Axis Gimbal LOS Rate Feedback Control Loop

 Copyright© 2019 Peter J. Kennedy

- **Azimuth rates to elevation rates (ω_{EY} obtained from RBE)**

$$\hat{\omega}_E(t)=\begin{bmatrix}\omega_{EX}(t)\\ \omega_{EY}(t)\\ \omega_{EZ}(t)\end{bmatrix}=\bar{R}_E(t)\hat{\omega}_A(t)+\hat{E}(t) \quad ; \quad \dot{\hat{E}}(t)=\begin{bmatrix}0\\ \dot{E}(t)\\ 0\end{bmatrix}$$

$$\dot{\hat{\omega}}_E(t)=\bar{R}_E(t)\dot{\hat{\omega}}_A(t)+\dot{\bar{R}}_E(t)\hat{\omega}_A(t)+\ddot{\hat{E}}(t)$$

$$\dot{\bar{R}}_E(t)\hat{\omega}_A(t)=\hat{\omega}_E(t)\times\dot{\hat{E}}(t) \qquad \text{x-cross-product}$$

$$\dot{\hat{\omega}}_E(t)=\bar{R}_E(t)\dot{\hat{\omega}}_A(t)+\hat{\omega}_E(t)\times\dot{\hat{E}}(t)+\ddot{\hat{E}}(t)$$

- **Platform rates to azimuth rates (ω_{AZ} obtained from RBE)**

$$\hat{\omega}_A(t)=\begin{bmatrix}\omega_{AX}(t)\\ \omega_{AY}(t)\\ \omega_{AZ}(t)\end{bmatrix}=\bar{R}_A(t)\hat{\omega}_P(t)+\dot{\hat{A}}(t) \quad ; \quad \dot{\hat{A}}(t)=\begin{bmatrix}0\\ 0\\ \dot{A}(t)\end{bmatrix}$$

$$\dot{\hat{\omega}}_A(t)=\bar{R}_A(t)\dot{\hat{\omega}}_P(t)+\dot{\bar{R}}_A(t)\hat{\omega}_P(t)+\ddot{\hat{A}}(t)$$

$$\dot{\bar{R}}_A(t)\hat{\omega}_P(t)=\hat{\omega}_A(t)\times\dot{\hat{A}}(t) \qquad \text{x-cross-product}$$

$$\dot{\hat{\omega}}_A(t)=\bar{R}_A(t)\dot{\hat{\omega}}_P(t)+\hat{\omega}_A(t)\times\dot{\hat{A}}(t)+\ddot{\hat{A}}(t)$$

Figure 17.0 Two -Axis Gimbal Kinematic Equations

The target vector is defined in inertial or NED coordinates, relative to the platform vehicle position. The vector is assumed as already derived from GPS position data. The relative NED target vector is rotated into the moving platform coordinates as:

$$\hat{P}_{TGTP}=D\bar{C}M^{P}_{NED}\cdot\hat{P}_{TGTNED}$$

The DCM in the equation is populated by the INS data providing the inertial orientation of the platform from which the target vector in platform coordinates can be determined. The vector in platform coordinates must be rotated through the gimbal coordinates to the LOS for determination of the required gimbal pointing angles as described in Section 3.0. The vector is rotated into inner elevation gimbal or LOS coordinates and used to obtain a pointing solution defined by the perfect pointing criterion:

$$\hat{P}_{TGTLOS}=\bar{R}_E\cdot\bar{R}_A\cdot\hat{P}_{TGTP} \quad \text{target in LOS coordinates.}$$

$$\text{For perfect pointing}: \hat{P}_{TGTLOS}=\begin{bmatrix}1\\0\\0\end{bmatrix}=\bar{R}_E\cdot\bar{R}_A\cdot\hat{P}_{TGTP} \quad \text{or} \ \therefore \ \bar{R}^T_A\cdot\bar{R}^T_E\cdot\begin{bmatrix}1\\0\\0\end{bmatrix}=\hat{P}_{TGTP}$$

As discussed in Section 3.0, the azimuth and elevation gimbal angles satisfying the condition for a perfect track are obtained as:

$$A_{CMD}=\text{atan}\left(\frac{P_{TGTPY}}{P_{TGTPX}}\right)$$

$$E_{CMD}=\text{atan}\left(\frac{-P_{TGTPZ}}{\sqrt{P_{TGTPX}+P_{TGTPY}}}\right)$$

These are then the command angle input to the pointing control loop to position the gimbal LOS to the target position. The servo control algorithm will not produce the exact angles, the vector zero components will actually contain errors or: $\hat{P}^T_{TGTLOS}=\begin{bmatrix}1 & e_{AZ} & e_{EL}\end{bmatrix}$. The last two vector components are azimuth and elevation LOS pointing errors nulled by the pointing servo loop. For this simple 2-axis gimbal example the sensor sight-line is aligned with the inner gimbal x-axis so

Copyright© 2019 Peter J. Kennedy

the gimbal LOS and sensor LOS are co-aligned. The complete control system block diagram for the example is shown in Figure 18.0; combining the rigid body with LOSR feedback (blue) and pointing/track loops (green). The gyros are mounted on elevation body directly measuring LOSR. The blocks with red print relate directly; the rigid body to the Figure 14.0, the servo rate loop feedback to Figure 16, rate kinematics to Figure 17.0 and finally the azimuth and elevation command angles generated using INS data as inputs to the pointing servo loop are shown. Once tracking, the LOS error is derived from camera and track algorithm.

Section 4.0 Key Points Summary

- ***Example for a two-axis system shows Rigid Body equations using principle inertias, off-axis inertias assumed equal to zero.***
- ***Kinematic angular rate equations derived and notional LOSR feedback control algorithm shown***
- ***Block diagram of expanded RBE provided; derived as a function of platform input disturbances and LOSR outputs show geometric interdependencies of rotation axes to LOS axes***
- ***Block diagram shown for RBE with LOSR control loop about the RB model***
- ***Block diagram of architecture for a complete SLC system; interfacing with a track sensor***

5.0 General Algorithm for Calculating the LOSR Vector [4, 5

The importance of LOSR in stabilizing the sightline has been described in Section 2.0. For simple 2-axis gimbal designs, if not measured directly deriving it from the kinematics of a sequence of rotation matrices may suffice. But for more complex systems this can sometimes be difficult. A more general algorithm is described in this section. As mentioned previously, the direction cosine matrix (DCM) describes the directional relationship between the coordinate frames attached to two rigid bodies A and B. The derivative of $D\bar{C}M_A^B$ is the product of this DCM and the skew-symmetric angular velocity matrix [ω x]. This equation, often termed the 'DCM kinematic equation', is defined as [3]:

$$D\dot{\bar{C}}M_A^B = -[\hat{\omega}\times]\cdot D\bar{C}M_A^B \qquad \text{where} \qquad [\hat{\omega}\times] \leftrightarrow \begin{bmatrix} 0 & -\omega_Z & \omega_Y \\ \omega_Z & 0 & -\omega_X \\ -\omega_Y & \omega_X & 0 \end{bmatrix}$$

Copyright© 2019 Peter J. Kennedy

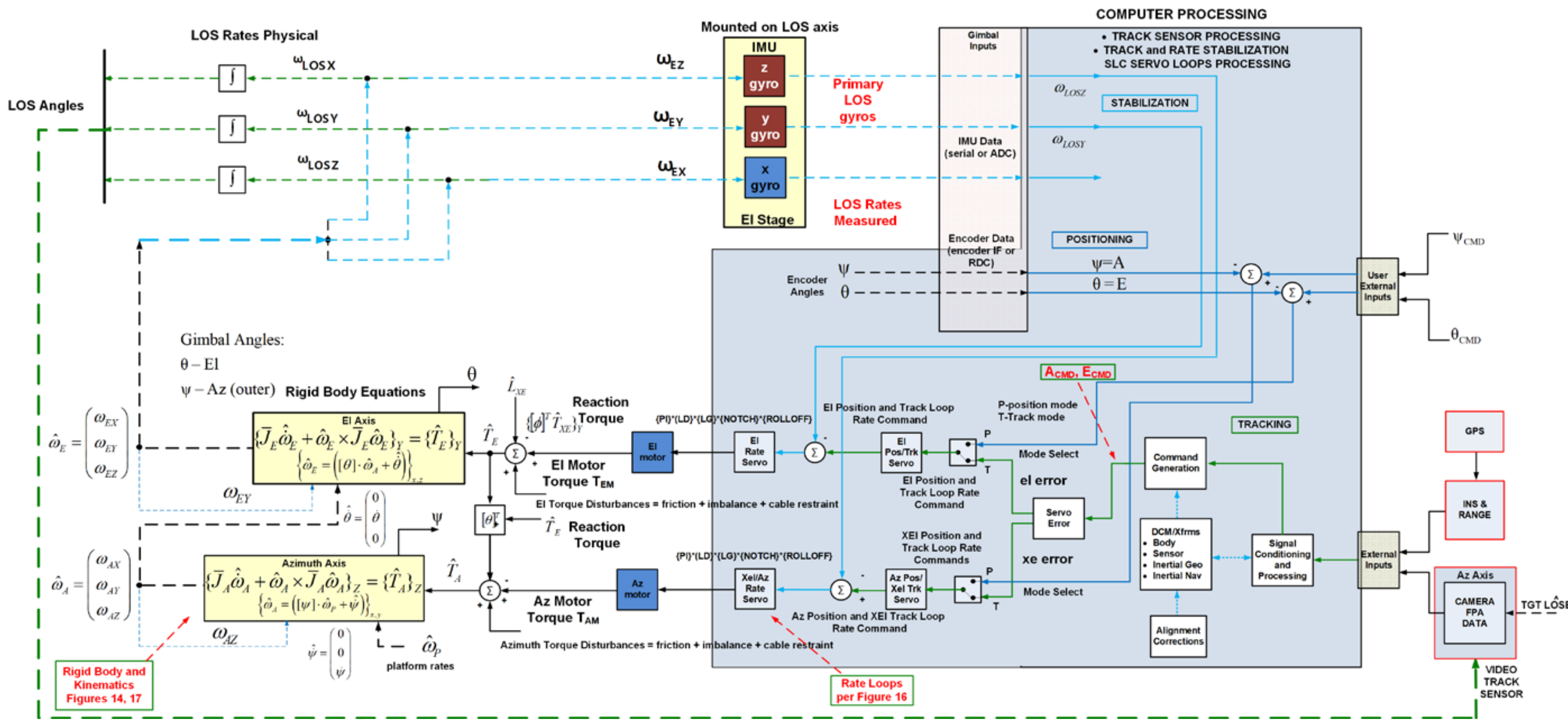

Figure 18.0 Two-Axis Gimbal SLC Control System Block Diagram for Geo-Pointing.

 Copyright© 2019 Peter J. Kennedy

Using this definition, one can define LOSR in terms of the derivative of a DCM from inertial to sensor LOS (SLOS) as: $D\dot{\bar{C}}M_I^{SLOS} = -\left[\hat{\omega}_{SLOS} \times\right] \cdot D\bar{C}M_I^{SLOS}$ and from inertial to platform as: $D\dot{\bar{C}}M_I^{P} = -\left[\hat{\omega}_{P} \times\right] \cdot D\bar{C}M_I^{P}$. The target vector in inertial coordinates is rotated into gimbal LOS coordinates by these two direction cosine matrices; inertial to platform $D\bar{C}M_I^P$ and platform to LOS $D\bar{C}M_P^{SLOS}$ as: $\hat{P}_{TGTLOS} = D\bar{C}M_P^{SLOS} \cdot D\bar{C}M_I^P \cdot \hat{P}_{TGTI}$. The key pointing relationship defining DCM partitioning and order is then:

$$D\bar{C}M_I^{SLOS} = D\bar{C}M_P^{SLOS} \cdot D\bar{C}M_I^P$$

$$\hat{P}_{TGTI} = \bar{R}^T(A_T) \cdot \bar{R}^T(El_T) \cdot \begin{bmatrix} 1 \\ 0 \\ 0 \end{bmatrix} \quad ; \quad D\bar{C}M_I^P = \bar{R}(roll_T) \cdot \bar{R}(pitch_P) \cdot \bar{R}(yaw_P)$$

To obtain an expression for LOSR, the equation for $D\bar{C}M_P^{SLOS}$ is differentiated. For those interested, the details are shown in Figure 19.0. A key equation obtained is shown in the first red-lined block as:

$$\left[\hat{\omega}_{SLOS} \times\right] \cdot D\bar{C}M_P^{SLOS} = -D\dot{\bar{C}}M_P^{SLOS} + \left[(D\bar{C}M_P^{SLOS} \cdot \hat{\omega}_P) \times\right] \cdot D\bar{C}M_P^{SLOS}$$

This expression is the sum of two terms; i) the derivative of the platform to gimbal DCM that will contain relative gimbal rates and ii) inertial to platform DCM derivative containing rotates platform rates. This general expression can be applied to many gimbal configurations. Continuing down the steps in Figure 19.0, the rotation matrix sequence for the 2 axis gimbal is defined as: $D\bar{C}M_P^{SLOS} = \bar{R}_E(t) \cdot \bar{R}_A(t)$ and the key equation algebraic operations shown in the figure to obtain a final expression for the LOSR vector as:

$$\hat{\omega}_{SLOS} = \bar{R}_E(t) \cdot \bar{R}_A(t) \cdot \hat{\omega}_P + \bar{R}_E(t) \cdot \dot{\hat{A}} + \dot{\hat{E}}$$

This expression is the same as derived in Section 3.0, since $\hat{\omega}_{SLOS} = \hat{\omega}_E$**,** by simply rotating the platform rate vector through the gimbal coordinate rotation matrices. However this approach derives rate from the pointing vector rotation sequence thereby relating the rate and pointing which can be applied to more complex configurations.

Copyright© 2019 Peter J. Kennedy

Using the definition of the inertial to the sensor LOS DCM derivative and differentiating the DCM product the following relationship is obtained: $D\dot{\bar{C}}M_I^{SLOS} = -[\hat{\omega}_{SLOS}\times]\cdot D\bar{C}M_I^{SLOS} = D\dot{\bar{C}}M_P^{SLOS}\cdot D\bar{C}M_I^P - D\bar{C}M_P^{SLOS}\cdot[\hat{\omega}_P\times]\cdot D\bar{C}M_I^P$

Substitute on the left for the definition of $D\bar{C}M_I^{SLOS}$ and post multiply through by $D\bar{C}M_I^P$ to obtain

$$[\hat{\omega}_{SLOS}\times]\cdot D\bar{C}M_P^{SLOS} = -D\dot{\bar{C}}M_P^{SLOS} + D\bar{C}M_P^{SLOS}\cdot[\hat{\omega}_P\times]$$

This expression is the sum of two terms; i) the derivative of the gimbal DCM that will contain relative gimbal rates and ii) a term that rotates platform rates into gimbal coordinates. This general expression can be applied to many gimbal configurations. The $D\bar{C}M_P^{SLOS}$ is unique to the gimbal configuration. Using the identity [4]: $D\bar{C}M_A^B\cdot[\hat{\omega}\times] = \left[(D\bar{C}M_A^B\cdot\hat{\omega})\times\right]\cdot D\bar{C}M_A^B$

The final form of the equation is:

$$[\hat{\omega}_{SLOS}\times]\cdot D\bar{C}M_P^{SLOS} = -D\dot{\bar{C}}M_P^{SLOS} + \left[(D\bar{C}M_P^{SLOS}\cdot\hat{\omega}_P)\times\right]\cdot D\bar{C}M_P^{SLOS}$$ **Key Equation**

Now for the 2-axis gimbal: $D\bar{C}M_P^{SLOS} = \bar{R}_E(t)\cdot\bar{R}_A(t)$ and $\dot{\bar{R}}_E(t) = -\left[\hat{\dot{E}}\times\right]\cdot\bar{R}_E(t)$; $\dot{\bar{R}}_A(t) = -\left[\hat{\dot{A}}\times\right]\cdot\bar{R}_A(t)$

Differentiate this equation, substitute, and use same identity $D\dot{\bar{C}}M_P^{SLOS} = -\left(\left[\hat{\dot{E}}\times\right] + \left[\left(\bar{R}_E(t)\cdot\hat{\dot{A}}\right)\times\right]\right)\cdot D\bar{C}M_P^{SLOS}$

Substitute into the Key Equation and pre-multiply by $D\bar{C}M_{SLOS}^P$: $[\hat{\omega}_{SLOS}\times] = \left[\hat{\dot{E}}\times\right] + \left[\left(\bar{R}_E(t)\cdot\hat{\dot{A}}\right)\times\right] + \left[(D\bar{C}M_P^{SLOS}\cdot\hat{\omega}_P)\times\right]$

Equating like elements of the skew symmetric matrix, the equation can be expressed in vector form as:

$$\hat{\omega}_{SLOS} = \hat{\dot{E}} + \bar{R}_E(t)\cdot\hat{\dot{A}} + \bar{R}_E(t)\cdot\bar{R}_A(t)\cdot\hat{\omega}_P$$ **2-Axis Gimbal LOSR**

Figure 19.0 Calculation of LOSR using DCM Kinematic Equation Approach

Section 5.0 Key Points Summary

- ***DCM between inertial coordinate frame and LOS coordinate frame used to derive LOSR for the two-axis gimbal example.***
- ***Key is division of DCM into two terms***
  - ***i) the gimbal DCM derivative will contain relative gimbal rates***
  - ***ii) a DCM that rotates inertial to platform coordinates***
- ***The LOSR equation derived is the same as in section 4.0 except this approach provides a generic format for more complex axis configurations***

6.0 LOS Kinematics with Mirrors [1, 2, 3, 5, 6, 7]

A LOS steering mirror has the advantage that the gimbal payload is effectively reduced to that of the mirror. This allows for a smaller gimbal design which has significant SWaP benefits for small platform pointing applications. Mirrors however have several unique characteristics that must be appreciated when designing a stabilized pointing system. As they are integrated with many pointing systems; these characteristics and how they might impact a geo-pointing design application are discussed.

1. When the LOS input to the mirror is perpendicular to the mirror rotation axis there is an optical angle gain (OAG), often 2:1, but can vary (i.e. √2:1) depending upon optical path

 Copyright© 2019 Peter J. Kennedy

geometry. With a two-axis elevation over azimuth configuration, the elevation axis rotation would have the 2:1 gain; meaning the reflected elevation LOS angle moves twice the mirror rotation angle. For stabilization, this means there is no physical mounting location for a gyro to measure the LOS angles or rates although they are still critical for stabilization. Control approaches to mitigate this issue are:

- Calculate LOS and LOSR from gyros or IMUs mounted on inner gimbal, outer gimbal, base, or combination thereof
- Secondary stable body (SB) mounted on a rotation axis parallel to the mirror axis; SB includes all gyros. Design for direct LOS control of the SB then couple SB angle to mirror through 2:1 drive; *mechanical:* pulley, *electrical:* resolver; *optical:* secondary mirror co-aligned with main mirror axis but on independent rotation axis that reflects optical transceiver signal on SB
- Do not steer about the mirror reflective axis; discussed next

2. If the LOS input is parallel to the mirror rotation axis; the 2:1 OAG issue on the rotation axis can be avoided. This configuration requires two fold mirrors with the final mirror directing the LOS at an offset from the outer gimbal rotation axis; also causing a parallax condition which could impact performance at short range. It also results in a larger geometry since two mirrors are necessary, but does mitigate the OAG.

3. Another mirror issue is that the LOS is defined by the bore-sight of a transceiver, located on the gimbal base or platform but steered by mirror(s) mounted on the inner axes.

   - When the platform moves relative to the mirror, so does the transceiver bore-sight. Platform rate couples directly into the disturbance error, as opposed to a normal mass stabilization problem where base motion (in elevation) is coupled only via friction, assuming a direct drive (i.e. no gears).
   - In addition, as the mirror, mounted on the inner axis rotates relative to the track sensor located at the base or outer axis the image rotates requiring image de-rotation electronically, in software, or mechanically (de-rotation prism)

4. LOSR is still the key to stabilization; calculating mirror LOSR for mirrors with a 2:1 OAG is discussed using the DCM approach, described previously, referenced to both sensor and gimbal LOS

The two mirror pointing geometries described above as characteristics 1.0 and 2.0, are shown in Figure 20.0. The left configuration has the 2:1 optical angle gain about the rotating axis, while the right side configuration does not.

 Copyright© 2019 Peter J. Kennedy

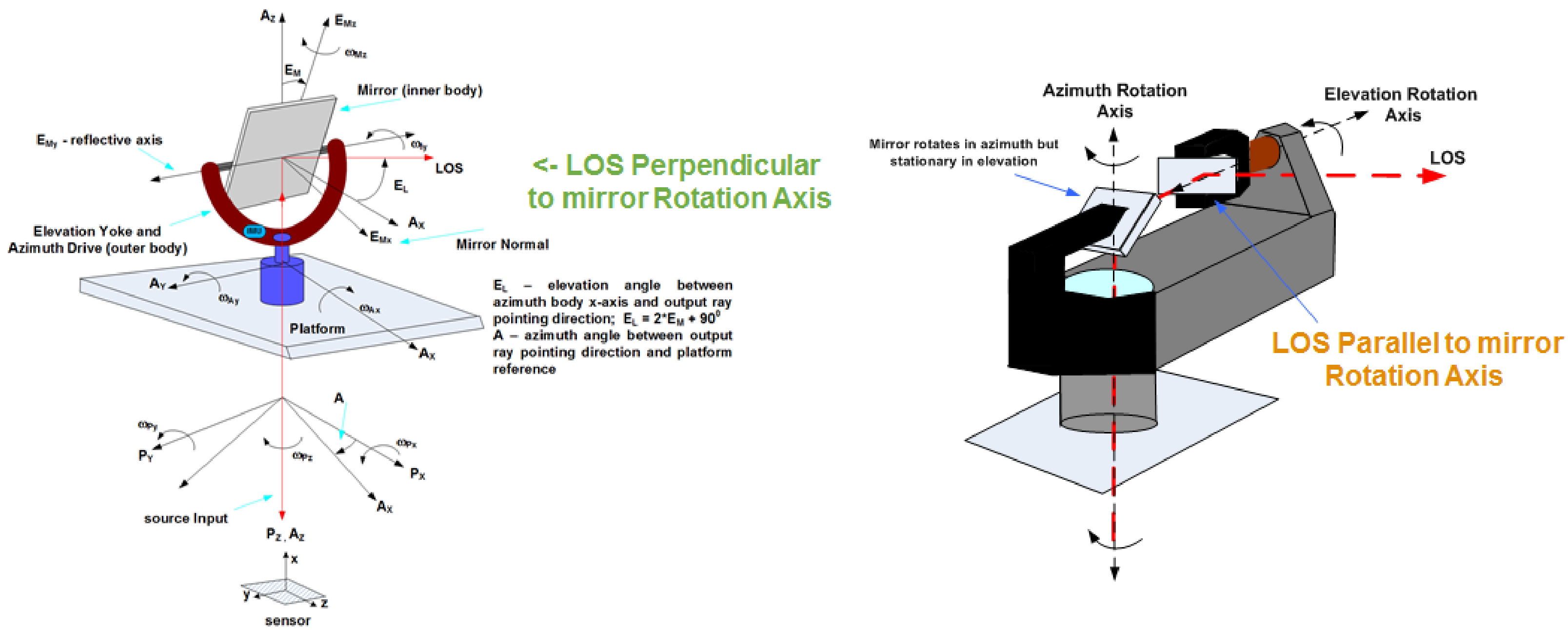

Figure 20.0 Two mirror rotation configurations; Left: simple El/Az with 2:1 OAG; Right: 2 mirror offset without OAG

 Copyright© 2019 Peter J. Kennedy

Direct LOS stabilization can be applied to the right side configuration, but the left configuration with the 2:1 OAG cannot be implemented directly. LOS disturbances are not directly measurable by simply mounting the rate sensors on this mirror structure. With a 2:1 mirror OAG, the mirror angle needs to move only half that of the disturbance. For this reason, the stabilization servo loop for a mirror with this OAG is often termed a half angle servo. The design will differ from a conventional gimbal servo system since there is no mechanical mirror structure appropriate for defining the LOS angle. The LOSR equations required for stabilization of a simple 2-axis el/az mirror assembly shown on the left side of Figure 20.0, are derived in this section. The DCM approach described in Section 5.0 is used. A difference with this design is that the gyros cannot be mounted directly on the LOS axes so the optical path rotation matrix sequence or DCM must account for the mirror reflective properties. To account for these properties, one approach is to define a reflection matrix for each reflective mirror element in the optical path. The method for generating the LOSR equations from the path DCM then closely follows that of Section 5.0. For the mirror configuration considered, the mirror is mounted to elevation shaft, the IMU mounted on azimuth rotation stage, and the sensor located in base on platform. A brief description and derivation of the reflection matrix is provided in Figure 21.0. The matrix is generated based upon the definition of the mirror normal and the general formula is shown within the red lined box at the top of the figure.

***Reflection Matrix:** Provides a general algorithm for rotating an input ray through mirror surface geometry to a reflected output ray*

$$\bar{M} = \begin{bmatrix} 1-2N_X^2 & -2N_X \cdot N_Y & -2N_X \cdot N_Z \\ -2N_Y \cdot N_X & 1-2N_Y^2 & -2N_Y \cdot N_Z \\ -2N_Z \cdot N_X & -2N_Z \cdot N_Y & 1-2N_Z^2 \end{bmatrix}$$

- **Reflection follows Snell's Law**
- **Incident beam, P_{IN}, fixed in the xyz system**
- **Reflected beam P_{OUT} exits the mirror surface at the same angle as the incident beam**
- **Incident beam reflected in LOS Rotation Plane relative to mirror normal $\hat{N}$**
- **The red arrows show incident and reflected beam vectors decomposed into components perpendicular and parallel to the normal vector**
- **The output and input vectors can be described by their components parallel (| |) and perpendicular (-|) components to the mirror normal $\hat{N}$**

output: $\hat{P}_{OUT} = \hat{P}_{OUT-|} + \hat{P}_{OUT\|}$; **input:** $\hat{P}_{IN} = \hat{P}_{IN-|} + \hat{P}_{IN\|}$

- **From the figure** $\hat{P}_{OUT} = \hat{P}_{IN-|} - \hat{P}_{IN\|}$
- **The parallel and perpendicular components of the input vector are (• – dot product):**

parallel: $\hat{P}_{IN\|} = (\hat{P}_{IN} \bullet \hat{N})\hat{N}$; **perpendicular:** $\hat{P}_{IN-|} = \hat{P}_{IN} - (\hat{P}_{IN} \bullet \hat{N})\hat{N}$

- **Substitute in the expression for P_{out} ->** $\hat{P}_{OUT} = \hat{P}_{IN} - 2(\hat{P}_{IN} \bullet \hat{N})\hat{N}$
- **Expand the equation for Pout, expressing it in matrix notation as:**

$$\hat{P}_{OUT} = \bar{M} \cdot \hat{P}_{IN} = \left\{ I - 2\begin{bmatrix} N_X \\ N_Y \\ N_Z \end{bmatrix}\begin{bmatrix} N_X & N_Y & N_Z \end{bmatrix} \right\} \hat{P}_{IN} = \begin{bmatrix} 1-2N_X^2 & -2N_X \cdot N_Y & -2N_X \cdot N_Z \\ -2N_Y \cdot N_X & 1-2N_Y^2 & -2N_Y \cdot N_Z \\ -2N_Z \cdot N_X & -2N_Z \cdot N_Y & 1-2N_Z^2 \end{bmatrix} \hat{P}_{IN}$$

where $\hat{N}^T = [N_X, N_Y, N_Z]$

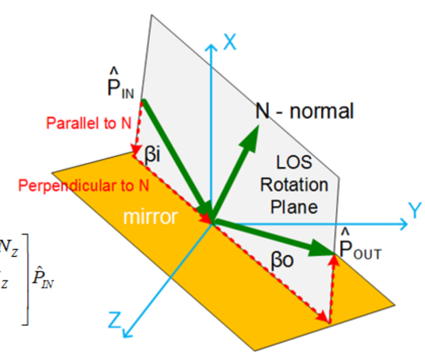

Figure 21.0 Reflection Matrix

For the two axis mirror configuration shown in Figure 20, the mirror rotation axis is elevation so the mirror rotates about its y-axis. There are several elevation angle (E) definitions. The mirror

Copyright© 2019 Peter J. Kennedy

elevation rotation angle is E_M=E+45°. The elevation LOS angle accounts for the 2:1 optical gain and is given by E_L=2*E=2*E_M+90°. With these definitions; the mirror axis rotation matrix and mirror normal vector are given by:

$$\bar{R}_{E_M} = \begin{bmatrix} c_{E_M} & 0 & -s_{E_M} \\ 0 & 1 & 0 \\ s_{E_M} & 0 & c_{E_M} \end{bmatrix} \quad \text{mirror rotation matrix}$$

$$\hat{N} = \bar{R}_{E_M}^T \cdot \begin{bmatrix} 1 \\ 0 \\ 0 \end{bmatrix} = \begin{bmatrix} c_{E_M} \\ 0 \\ -s_{E_M} \end{bmatrix} \quad \text{mirror normal unit vector}$$

Using this definition of the mirror normal vector, the reflection matrix is then derived as:

$$M = \begin{bmatrix} 1-2\cdot c_{E_M}{}^2 & 0 & 2\cdot c_{E_M}\cdot s_{E_M} \\ 0 & 1 & 0 \\ 2\cdot c_{E_M}\cdot s_{E_M} & 0 & 1-2\cdot s_{E_M}{}^2 \end{bmatrix} = \begin{bmatrix} -c_{2\cdot E_M} & 0 & s_{2\cdot E_M} \\ 0 & 1 & 0 \\ s_{2\cdot E_M} & 0 & c_{2\cdot E_M} \end{bmatrix} = \begin{bmatrix} -s_{E_L} & 0 & -c_{E_L} \\ 0 & 1 & 0 \\ -c_{E_L} & 0 & s_{E_L} \end{bmatrix}$$

This calculation is the main difference between the 2-axis gimbaled mirror and simple 2-axis gimbal LOSR derivation. For the mirror derivation, there is also a slight difference in LOS definition at the sensor and in gimbal coordinates due to the image roll at the sensor as described earlier. For the mirror configuration in Figure 20.0. With the sensor (S) mounted to the base or platform, the rotation of a target vector in inertial coordinates to the sensor coordinate frame provides the LOS at the sensor following the rotation sequence:

$$\hat{P}_{SLOS} = \bar{R}_S \cdot \bar{R}_A^T(t) \cdot \bar{M}(t) \cdot \bar{R}_A \cdot D\bar{C}M_I^P \cdot \hat{P}_{TI}$$

$$\text{where the sensor orientation matrix } \bar{R}_S = \begin{bmatrix} 0 & 0 & -1 \\ 0 & 1 & 0 \\ -1 & 0 & 0 \end{bmatrix}$$

$$\text{and as previously defined } D\bar{C}M_I^P = \bar{R}(roll_T) \cdot \bar{R}(pitch_P) \cdot \bar{R}(yaw_P)$$

Sequence terms can be combined into those for LOS rotation and the image roll on the sensor due to azimuth rotation that are more meaningful to the optical path as:

$$\hat{P}_{SLOS} = \left\{ \bar{R}_{Ar}^T(t) \cdot \bar{R}_{LOS} \cdot \bar{R}_A \right\} \cdot D\bar{C}M_I^P \cdot \hat{P}_{TI}$$

$$\text{where } \bar{R}_{LOS} = \bar{R}_S \cdot \bar{M}(t) \quad \text{LOS rotation matrix}$$

$$\text{and } \bar{R}_{Ar}(t) = \bar{R}_S \cdot \bar{R}_A^T(t) \cdot \bar{R}_S^T = \begin{bmatrix} 1 & 0 & 0 \\ 0 & c_A & s_A \\ 0 & -s_A & c_A \end{bmatrix} \quad \text{matrix for image roll}$$

Copyright© 2019 Peter J. Kennedy

Similar to the 2-axis gimbal example, the sequence is segmented into two direction cosine matrices, one from inertial coordinates to the platform and the other from the platform frame to sensor coordinates.

$$\hat{P}_{SLOS} = D\bar{C}M_{I}^{SLOS} \cdot \hat{P}_{TI} = D\bar{C}M_{P}^{SLOS} \cdot D\bar{C}M_{I}^{P} \cdot \hat{P}_{TI}$$

where $D\bar{C}M_{I}^{SLOS} = D\bar{C}M_{P}^{SLOS} \cdot D\bar{C}M_{I}^{P}$ and $D\bar{C}M_{P}^{SLOS} = \bar{R}_{Ar}^{T}(t) \cdot \bar{R}_{LOS}(t) \cdot \bar{R}_{A}(t)$

From this point forward, the derivation follows that described in Section 5.0 and is outlined in Figure 22.0.

- **Following the 2-axis gimbal example for the DCM derivative**

$$D\dot{\bar{C}}M_{I}^{SLOS} = -[\hat{\omega}_{SLOS}\times] \cdot D\bar{C}M_{I}^{SLOS} = -[\hat{\omega}_{SLOS}\times] \cdot D\bar{C}M_{P}^{SLOS} \cdot D\bar{C}M_{I}^{P} = D\dot{\bar{C}}M_{P}^{SLOS} \cdot D\bar{C}M_{I}^{P} + D\bar{C}M_{P}^{SLOS} \cdot D\dot{\bar{C}}M_{I}^{P}$$

- **Substituting** $D\dot{\bar{C}}M_{I}^{P} = -[\hat{\omega}_{P}\times] \cdot D\bar{C}M_{I}^{P}$ ***results in the baseline expression below; note similarity to 'Key Equation' slide 37:***

$$[\hat{\omega}_{SLOS}\times] \cdot D\bar{C}M_{P}^{SLOS} = -D\dot{\bar{C}}M_{P}^{SLOS} + \left[(D\bar{C}M_{P}^{SLOS} \cdot \hat{\omega}_{P})\times\right] \cdot D\bar{C}M_{P}^{SLOS}$$

General Equation LOSR at Sensor

- ***Using the DCM definitions, the derivative*** $D\dot{\bar{C}}M_{P}^{SLOS}$ **can be derived after several steps as:**

$$D\dot{\bar{C}}M_{P}^{SLOS} = -\left(\dot{A} \cdot [-\hat{u}_{x}\times] + \left[\left(\bar{R}_{Ar}^{T}(t) \cdot \hat{\dot{E}}_{L}\right)\times\right] + \left[\left(\bar{R}_{Ar}^{T}(t) \cdot \bar{R}_{LOS}(t) \cdot \hat{\dot{A}}\right)\times\right]\right) \cdot D\bar{C}M_{P}^{SLOS}$$

- **Substituting into the general equation for LOSR at Sensor:**

$$[\hat{\omega}_{SLOS}\times] = \dot{A} \cdot [-\hat{u}_{x}\times] + \left[\left(\bar{R}_{Ar}^{T}(t) \cdot \hat{\dot{E}}_{L}\right)\times\right] + \left[\left(\bar{R}_{Ar}^{T}(t) \cdot \bar{R}_{LOS}(t) \cdot \hat{\dot{A}}\right)\times\right] + \left[(D\bar{C}M_{P}^{SLOS} \cdot \hat{\omega}_{P})\times\right]$$

- **Combining the last two terms and expressing in vector format:**

$$\hat{\omega}_{SLOS} = -\dot{A} \cdot \hat{u}_{x} + \bar{R}_{Ar}^{T}(t) \cdot \hat{\dot{E}}_{L} + \bar{R}_{Ar}^{T}(t) \cdot \bar{R}_{LOS}(t) \cdot \hat{\omega}_{A}$$

2-Axis Mirror LOSR at Sensor

- **This expression provides the LOSR at the sensor accounting for image rotation.** ***To obtain the gimbal LOSR aligned to the gimbal axes as for the first example, multiply by the transpose of the image rotation matrix to obtain:***

$$\hat{\omega}_{LOS} = \bar{R}_{Ar} \cdot \left(-\dot{A} \cdot \hat{u}_{x} + \bar{R}_{Ar}^{T}(t) \cdot \hat{\dot{E}}_{L} + \bar{R}_{Ar}^{T}(t) \cdot \bar{R}_{LOS}(t) \cdot \hat{\omega}_{A}\right)$$

$$\hat{\omega}_{LOS} = -\dot{A} \cdot \hat{u}_{x} + \hat{\dot{E}}_{L} + \bar{R}_{LOS}(t) \cdot \hat{\omega}_{A}$$

- ***The final expression for the LOSR vector components is given by:***

$$\hat{\omega}_{LOS} = \begin{bmatrix} -\dot{A} + c_{E_L} \cdot \omega_{AX} - s_{E_L} \cdot \omega_{AZ} \\ 2 \cdot \dot{E} + \omega_{AY} \\ c_{E_L} \cdot \omega_{AZ} + s_{E_L} \cdot \omega_{AX} \end{bmatrix}$$

2-Axis Mirror LOSR at Gimbal LOS

Figure 22.0 Calculation of Mirror LOSR using DCM Kinematic Equation Approach

Copyright© 2019 Peter J. Kennedy

Section 6.0 Key Points Summary

- ***Mirrors are important in SLC as they provide for the use of large sensor suites with less pointing gimbal SWaP and better pointing performance.***
- ***They have unique characteristics that must be addressed to achieve their performance potential; including optical angle gain, image rotation; and direct platform disturbance coupling***
- ***The reflection matrix provides a general algorithm for rotating an input ray through mirror surface geometry to an output ray***
- ***The DCM approach from section 5.0 to generate LOSR is applied to a two-axis steering mirror geometry to obtain its LOSR vector***

7.0 LOS Pointing Control Design Components

A very brief overview of key components required by a gimbal system for geo-pointing

- Inertial Angular Motion

Inertial motion sensors – Gyro; Inertial Measurement Unit (IMU), Inertial Navigation system (INS). Gyros and IMU measure inertial angular rate. Performance ranges from commercial to tactical to navigation quality. Types include Spinning mass, fiber optic gyro (FOG), ring laser gyro (RLG), MEMS rate sensors, magnetic hydrodynamic rate sensor, and hemispherical resonator gyro. Types summarized as:

- gyros-measure inertial angular rate; configured in single axis, two-axis, and three-axis versions
- inertial measurement unit (IMU) – 3 gyros mounted on three orthogonal axes (i.e. x, y, z) measure rate about each respective axis and 3 accelerometers mounted on each axis measure acceleration along each axis
- Inertial navigation system (INS)-measures inertial angular position, and with GPS, location. It is effectively an IMU with integrated outputs and navigation algorithms (i.e. Extended Kalman Filter - EKF)

- For many applications, especially requiring geo-positioning an INS is mounted to the platform (possibly comes with the platform) and an IMU or set of gyros are mounted on gimbal or at its base. In general the gyro and IMU have much higher bandwidth and sampling rate than the INS as the INS needs time effectively process data in the EKF. However if the INS and IMU are aligned; accurate inertial angle data from the INS can be blended with integrated rate data from the IMU to update the effective inertial angles between INS sample substantially improving geo-positioning performance. The alignment

 Copyright© 2019 Peter J. Kennedy

between INS and IMU is often termed transfer alignment and can be performed during operation at a time interval consistent with the sensor noise characteristics.

- Gyro and IMU (gyro and accelerometers) error sources that can corrupt the geo-location estimate are drift and angular random walk (ARW). Drift is usually considered a bias, but may have short and long term components. ARW is considered a random disturbance error associated with the INS gyros and accelerometers. The magnitude of the random error vary significantly with the sensor quality. ARW is effectively the result of integrating the gyro white noise. Random walk can be described by the differential equation dx/dt= η where η is a white noise term with PSD N. Drift is effectively a constant bias angular rate on the output of a gyro, independent of the input. It is an offset rate that will not change during a short run, but may vary from turn-on to turn-on or over longer periods. Another gyro error is the scale factor error which is in general a linear error that is proportional to the input signal; however it may exhibit some degree of non-linearity over the full scale sensor range.

- Inertial errors can vary significantly depending on the quality of the inertial sensors. Drift and bias in tactical grade sensors is usually high. Heading can be difficult to measure without an inertial grade INS/GPS. Tactical grade inertial sensors often use a magnetometer that provides heading relative to magnetic north which can be corrected for true north given latitude and longitude. However magnetometers measurements are corrupted by externally induced magnetic fields. Differential GPS is another method to obtain heading; accuracy being dependent on the separation distance between two GPS antennas. In addition, as the heart of an INS is an IMU, many of the IMU errors can be modeled by random white noise and Markov processes and included in a navigation error model implemented within an Extended Kalman Filter that significantly reduces their impact on the final solution.

- The performance of low quality inertial sensors can sometimes be improved if referenced to an inertial grade sensor co-located on the same structure. This s another advantage of transfer alignment mentioned above; using information from the reference system to align low quality inertial sensors on the platform. The algorithms use velocity or velocity integral matching to align accelerometers and gyro rate as will be shown in the next section.

- <u>Relative Angle Position Sensors</u>
  - Resolvers: construction similar to motor, rotor and stator coils produce sine/cosine signals from whose phase angle is determined, absolute angle measurement, wide angle range 360°, use multi-speed for high accuracy down to ~10 micro-radians (urad)
  - Encoders:

 Copyright© 2019 Peter J. Kennedy

- Relative encoders: bar type pattern generates pulse sequence whose count provides angle relative to a reference, when power is lost lose count, must reset wide angle range 360° ,very accurate with interpolation algorithms
- Absolute encoders: similar to resolver, maintains count even if power is lost , provide wide angle range 360°

- Other position sensor types; potentiometer, hall effect, capacitive, inductive most tend to have limited angle coverage, less accuracy

- Motors

  - Recommend direct drive (brush or brushless) for LOS stabilization applications to benefit from load inertia; also cog-less with low ripple torque
  - Brushless DC (BLDC) direct drive motors need to commutate with hall effect sensors, resolver, or encoder
  - Brush DC direct drive, simpler to implement, downside brush friction, sparking concerns in explosive atmosphere and brush wear. For many applications gimbals do not run continuously at high RPM so wear may be minimal and friction often less than bearing friction
  - Gear or belt driven motor drives are not recommended as they directly couple to a base and have resonance issues
  - For small payload and limited angle applications with low load inertia one can consider motors or other motion control actuator devices that provide very high BW response, compensating for low inertia.
    - Limited angle rotary torque motors
    - Friction drive piezoelectric
    - Fast Steering Mirrors (FSM) high BW limited travel
    - Voice coil actuators (VCA)

Section 7.0 Key Points Summary

- ***A brief description of key hardware components required to implement a SLC system is provided***
- ***Inertial rate and position sensors: gyro, IMU, INS.***
- ***Angle measurement sensors: resolvers, encoders***
- ***Motors: direct drive and limited angle actuators***

Copyright© 2019 Peter J. Kennedy

8.0 Geo-Pointing

Accurate pointing, briefly discussed in Section 3.0, provides the means to geo-locate or estimate the geographic location of an objects position by determining its geographic coordinates. A geo-location is defined based upon the latitude and longitude coordinates of a particular location and may be enhanced further by cross referencing or mapping to other type of address information depending on the application. This section describes the process of geo-pointing to locate a point-like object based upon the location and orientation of a pointing platform. The geo-pointing vector for location will require several coordinate frames of reference which may include sensor LOS, gimbal orientation, and the final geo-location reference frame. The actual coordinate frames will be application dependent. Defining the rotation matrices and the direction cosine matrices for each reference coordinate frame is key to determining a geographic location. Quaternions are another approach to representing the DCM. As the derivative of quaternion elements are a set of time varying linear differential equations, their values are easily obtained via integration. Quaternion rotation algorithms are readily available as self-contained CAD processing blocks; however quaternions will not be discussed further in this course.

For a geo-pointing application, one may assume the platform position is known and a targeted objects position at some known range needs to be determined. An optical or RF sensor mounted on the platform may be used to determine target angular position relative to the platform if not known. The sensor is mounted on a 2-axis gimbal, as described in previous sections of the course. The sensor could be part of a sensor network, surveillance or security, so that an objects position must be known in a coordinate frame common to the sensor network. The other major platform sensors are the gimbal angular position sensors, an IMU for stabilization, an INS for platform inertial orientation, and a GPS. The target location is initially measured in a sensor line of sight (LOS) frame, converted to a position vector, and must then be transferred to the common frame. The target vector is then rotated sequentially through each DCM, briefly described in Section 3.0 and again below, to obtain its position in the common frame. For the example, a gimbal mounted sensor is secured to a vehicle and would have coordinate frames that define the: sensor, gimbal, platform body, local surface referenced north east down, and finally the geo-location frame. The most often used geo-location frames are earth centered earth fixed (ECEF) and earth centered inertial (ECI). The ECEF frame is more often used for representing position and velocity of terrestrial objects while ECI for satellite applications specifying celestial objects location. The remainder of this course will assume the use of ECEF coordinates and a set of 5 coordinate frames, often used and illustrated in Figure 23.0, is as follows:

 Copyright© 2019 Peter J. Kennedy

https://www.pexels.com/photo/quadcopter-flying-on-the-skey-1034812/ archived on 20 May 2018 at the Wayback Machine

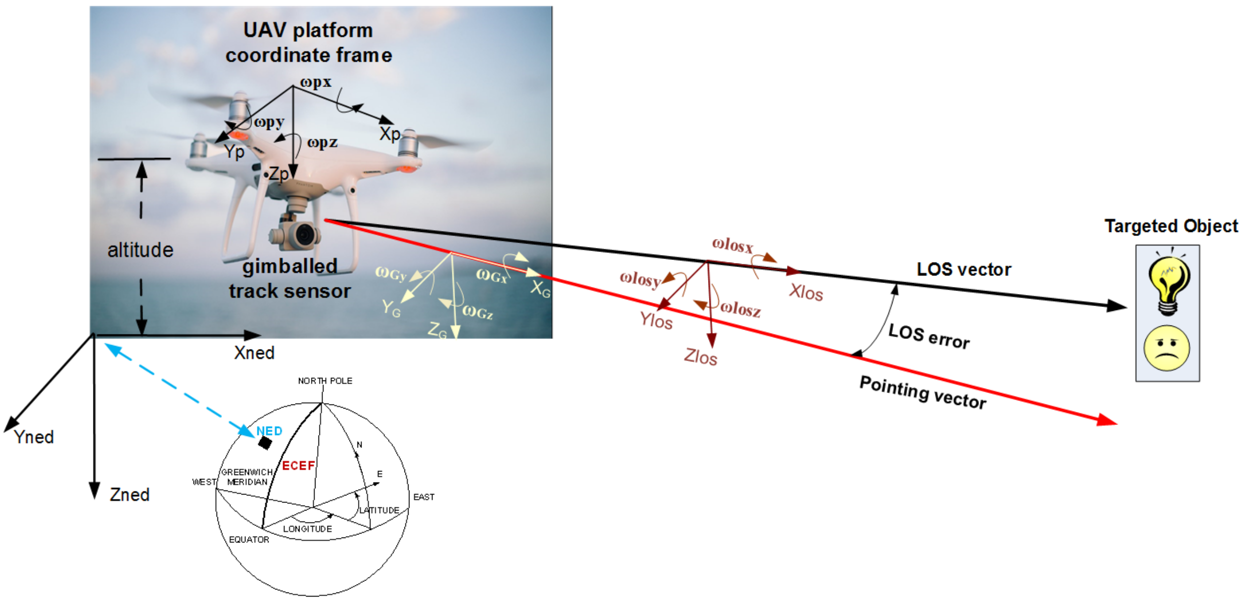

Figure 23.0 Typical coordinate frame geometry for geo-location

- (i) Earth-Centered, Earth-Fixed (ECEF)
  - The ECEF coordinate frame is a spherical earth model with the origin at the center of the Earth (Earth-Centered) and that rotates with the Earth (Earth-fixed)
  - The z-axis through the North Pole
  - The x axis through the Greenwich Meridian
  - The y axis completing a right-handed coordinate frame.
  - Latitude, longitude, and altitude location maps to ECEF position vector
- (ii) North East Down (NED)
  - Also termed inertial reference or local level
  - Platform/sensor pointing reference location
  - X axis points north orthogonal to gravity, Y axis points east orthogonal to gravity, and Z axis down co-linear with gravity
- (iii) Platform coordinate frame
  - Heading is about the NED Z axis (~down)
  - Pitch is about the new Y axis,
  - Roll is about the new X axis, with right hand rule for positive rotation
- (iv) Gimbal coordinate frame
  - Azimuth is about z-axis orthogonal to base mounting plane (~down)

Copyright© 2019 Peter J. Kennedy

    - elevation is about the new Y axis,
    - Roll is about the new X axis, with right hand rule for positive rotation
  - (v) Line-of-Sight (LOS) frame
    - X axis out the LOS, Y axis to the right when looking forward and Z axis down, with right hand rule for positive rotation
    - If a mirror is used, need to develop LOS and image kinematics

Using ECEF coordinates, an objects earth-centered location can be defined as a position in terms of latitude, longitude, and altitude relative to an ellipsoidal Earth model referenced to the World Geodetic System (WGS) 84 datum. The LOS coordinate frame defines the sensor bore sight relative to the LOS. With the sensor mounted on the inner gimbal structure, it is aligned to the gimbal axes. The gimbal frame defines the gimbal orientation relative to the platform body. The body coordinate frame is attached to the platform and often uses standard aircraft coordinates with the x-axis along the platform longitudinal axis, the z-axis pointing down orthogonal to the x-axis, and the y-axis oriented to complete a right handed coordinate system. The body coordinate frame is easily referenced to a north east down coordinate (NED) frame, sometimes referred to as a flat earth or local level model and in context of prior sections of this course was the inertial frame. An INS provides measurements relative to true or magnetic north (heading) and gravity (pitch and roll). The NED frame is then referenced to ECEF coordinates based upon latitude and longitude. For the example, with the gimbaled sensor configuration, the relative target position vector measured in the sensor LOS coordinate frame would rotate through the following sequence of 4 DCMs to obtain its orientation in the ECEF frame:

$$D\bar{C}M_{LOS}^{ECEF} = D\bar{C}M_{NED}^{ECEF}\left(\Phi_P,\Lambda_P\right)\cdot D\bar{C}M_{PLAT}^{NED}\left(\omega,\theta,\psi\right)\cdot D\bar{C}M_{GIMBAL}^{PLAT}\left(\alpha,\beta\right)\cdot D\bar{C}M_{LOS}^{GIMBAL}\left(\varepsilon x,\varepsilon y\right)$$

The notation uses a 'hat' to denote a matrix and a 'tilde' a vector. The subscript associated with a DCM denotes the source (from) coordinate frame while the superscript the destination (to) coordinate frame. Angles are defined as follows:

Φ_P: platform geodetic latitude (WGS84)
Λ_P: platform longitude (WGS84)
θ : platform pitch (platform INS)
ω : platform roll (platform INS)
ψ : platform heading (platform INS)
α : azimuth (gimbal)
β : elevation (gimbal)
Δx: measured sensor LOS x-target offset from center
εx = pixel Δx*$IFOV_{sensor}$ (for a camera)
Δy: measured sensor LOS y-target offset from center
εy = pixel Δy*$IFOV_{sensor}$ (for a camera)

Copyright© 2019 Peter J. Kennedy

Each DCM is the product of two or three rotations defined as:

$$D\bar{C}M_{LOS}^{GIMBAL}(\varepsilon x,\varepsilon y)=\begin{bmatrix}\cos(\varepsilon x) & -\sin(\varepsilon x) & 0\\ \sin(\varepsilon x) & \cos(\varepsilon x) & 0\\ 0 & 0 & 1\end{bmatrix}\cdot\begin{bmatrix}\cos(\varepsilon y) & 0 & \sin(\varepsilon y)\\ 0 & 1 & 0\\ -\sin(\varepsilon y) & 0 & \cos(\varepsilon y)\end{bmatrix}$$

$$D\bar{C}M_{GIMBAL}^{PLAT}(\alpha,\beta)=\begin{bmatrix}\cos(\alpha) & -\sin(\alpha) & 0\\ \sin(\alpha) & \cos(\alpha) & 0\\ 0 & 0 & 1\end{bmatrix}\cdot\begin{bmatrix}\cos(\beta) & 0 & \sin(\beta)\\ 0 & 1 & 0\\ -\sin(\beta) & 0 & \cos(\beta)\end{bmatrix}$$

$$D\bar{C}M_{PLAT}^{NED}(\omega,\theta,\psi)=\begin{bmatrix}\cos(\psi) & -\sin(\psi) & 0\\ \sin(\psi) & \cos(\psi) & 0\\ 0 & 0 & 1\end{bmatrix}\cdot\begin{bmatrix}\cos(\theta) & 0 & \sin(\theta)\\ 0 & 1 & 0\\ -\sin(\theta) & 0 & \cos(\beta)\end{bmatrix}\cdot\begin{bmatrix}1 & 0 & 0)\\ 0 & \cos(\omega) & -\sin(\omega)\\ 0 & \sin(\omega) & \cos(\omega)\end{bmatrix}$$

$$D\bar{C}M_{NED}^{ECEF}(\Phi_P,\Lambda_P)=\begin{bmatrix}\cos(\Lambda_P) & -\sin(\Lambda_P) & 0\\ \sin(\Lambda_P) & \cos(\Lambda_P) & 0\\ 0 & 0 & 1\end{bmatrix}\cdot\begin{bmatrix}\cos(\Phi_P) & 0 & -\sin(\Phi_P)\\ 0 & 1 & 0\\ \sin(\Phi_P) & 0 & \cos(\Phi_P)\end{bmatrix}\cdot\begin{bmatrix}0 & 0 & -1\\ 0 & 1 & 0\\ 1 & 0 & 0\end{bmatrix}$$

The geo-pointing problem is locating a target vector in ECEF coordinates, given a target range measurement. The target vector is the sum of the platform position in ECEF coordinates plus the measured relative target position vector, or:

$$\hat{P}_{TGT}^{ECEF}=\hat{P}_{PLAT}^{ECEF}+range\cdot D\bar{C}M_{LOS}^{ECEF}\begin{bmatrix}1\\0\\0\end{bmatrix}$$

The DCM is determined based upon the measured gimbal angles, INS, and GPS data. Range equates to distance. For a short distance between platform and target (flat earth model applies), measurable with a rangefinder or triangulation, range is often used. For longer distances dependent on the earth curvature, models that account for curvature and obtain distance from differences in latitude and longitude are required; as will be discussed in Part 2 of the course. Platform position in ECEF Cartesian coordinates is obtained from the vehicle geodetic latitude, longitude, and altitude as:

Copyright© 2019 Peter J. Kennedy

$$\hat{P}_{PLAT}^{ECEF} = \begin{bmatrix} \left(\dfrac{R_{EQ}}{\sqrt{1-e^2\cdot\sin^2(\Phi)}}+\text{altitude}\right)\cdot\cos(\Phi)\cdot\cos(\Lambda) \\ \left(\dfrac{R_{EQ}}{\sqrt{1-e^2\cdot\sin^2(\Phi)}}+\text{altitude}\right)\cdot\cos(\Phi)\cdot\sin(\Lambda) \\ -\left(\left(\dfrac{R_{PL}}{R_{EQ}}\right)^2\cdot\dfrac{R_{EQ}}{\sqrt{1-e^2\cdot\sin^2(\Phi)}}+\text{altitude}\right)\cdot\sin(\Phi) \end{bmatrix}$$

Where the earth's semi-major axis R_{EQ} = 20, 925, 646 feet (earth's radius at equator), R_{PL}=20, 850, 147.59 (earths radius at pole) and the square of the earth's eccentricity e^2 = 0.00669438. To obtain the ECEF angular coordinates of the target, longitude can be obtained as:

$$\Lambda_T = \tan^{-1}\left(\frac{P_{TGTX}^{ECEF}}{P_{TGTY}^{ECEF}}\right)$$

There is not a direct solution for geodetic latitude but it can be determined iteratively with an initial estimate as:

$$\Phi_T \approx \tan^{-1}\left(\frac{P_{TGTZ}^{ECEF}}{\sqrt{(P_{TGTX}^{ECEF})^2+(P_{TGTY}^{ECEF})^2}}\right)$$

There are also converters available on the internet that will do the x, y, z to latitude, longitude, altitude conversion such as: https://www.mathworks.com/matlabcentral/fileexchange/7941-convert-cartesian-ecef-coordinates-to-lat-lon-alt. However as this is obtained from an iterative estimate there will be an associated error. This completes Part 1 of the course with a more in-depth discussion of geo-pointing and locating in Part 2.

Summary Section 8.0 Key Points

- ***Definition of key coordinate frames used for geo-pointing are provided***
- ***The DCM sequence between ECEF coordinates and LOS coordinates is shown***
- ***The geo-pointing vector between a geo-referenced platform location and a target location is derived.***

9.0 Course Summary

Part 1 of the course has reviewed sightline control architecture, in general, and with application to geo-pointing. Section 1.0 covered LOS definition, methodology to characterize disturbances in terms of bias and jitter and performance metrics to evaluate the disturbance rejection requirements. Section 2.0 LOS Control Architecture and stabilization techniques. Section 3.0 LOS Control of

 Copyright© 2019 Peter J. Kennedy

the Rigid Body Dynamics, LOS Kinematics. Section 4.0 a 2-Axis Gimbal Example. Section 5.0 General Algorithm for Deriving LOSR. Section 6.0 LOS Control using mirrors. Section 7.0 provides a very brief discussion of key LOS control components. Finally Section 8.0 describes the initial aspects specific to geo-pointing and locating.

References

1. Rue, A.K. ”Stabilization of Precision Electro Optical Pointing and Tracking Systems”, IEEE Transactions on Aerospace and Electronic Systems, AES-5 No. 5, 805-819, September 1969
2. Rue, A.K. ”Precision Stabilization Systems”, IEEE Transactions on Aerospace and Electronic Systems, AES-10 No. 1, 34-42, January 1974
3. Kennedy, P., Kennedy, R., Stabilizing the Line of Sight , ISBN: 978-0-9988539-7-0; 978-1-7320721-0-7, Laurin Publishing/Photonics Media Press, April 6 2018 (www.lineofsightstabilization.com)
4. Kane Thomas R., Likins, Peter W., Levinson, David A., Spacecraft Dynamics, McGraw Hill Book Company, 1993 manuscript now freely available from the Internet-First University Press repository within DSpace at Cornell University at: http://dspace.library.cornell.edu/handle/1813/62
5. “Line of Sight Kinematics for a Two-Axis Head Mirror: Equations for Predicting and Controlling Mirrored LOS Pointing”, James M.B. Royalty, Proc. SPIE 7338 Acquisition, Tracking, Pointing, and Laser Systems Technologies XXIII, 733804 (4 May 2009); doi: 10.1117/12.818893
6. “Line-of-Sight Kinematics and Corrections for Fast Steering Mirrors used in Precision Pointing and Tracking Systems”, J.M. Hilkert, Proc. SPIE Vol. 9076, 90760F6, F7 (July 2014)
7. “A comparison of inertial line-of-sight stabilization techniques using mirrors”, J.M. Hilkert, Proc. SPIE 5430338 Acquisition, Tracking, Pointing XVIII, 0277-786X/04 (May 2004); doi: 10.1117/12.541808

Copyright© 2019 Peter J. Kennedy